WESTINGHOUSE CLASS 3 (Non-Proprietary)

[redacted]

WESTINGHOUSE CLASS 3 (Non-Proprietary)

[redacted]

Westinghouse Energy Systems

WCAP-13603

RV Closure Head Penetration Alloy 600 PWSCC (Phase 2)

December 1992

WESTINGHOUSE ELECTRIC CORPORATION
Nuclear and Advanced Technology Division
P.O. Box 355
Pittsburgh, Pennsylvania 15230

WPF0746A:1b/010593

TABLE OF CONTENTS

Section		Page
Table of Contents		i
List of Figures		iii
List of Tables		vi
Executive Summary		vii
1.0 Introduction		1
2.0 Penetration Stress Analysis		2
	2.1 Background	2
	2.2 Approach	2
	2.3 Elastic-Plastic Analysis Procedure	3
	2.4 Stress Analysis Results – Outermost Penetration	7
	2.5 Stress Analysis Results – Intermediate Penetration	13
	2.6 Stress Analysis Results – Center Penetration	13
	2.7 Reactor Vessel Head Bolt-up Stress Contribution	18
	2.8 ASME Code/Reactor Vessel Head to Penetration Tube Weld Conservatism	27
	2.9 Development of Stress/Strain Curves	33
	2.10 Two and Three-Loop Reactor Vessel Reconciliation	46
	2.11 Summary and Conclusions	50
3.0 Crack Growth Analysis: Flaw Tolerance		52
	3.1 Introduction	52
	3.2 Crack Growth Prediction Methodology	52
	3.3 Overall Approach	54
	3.4 Results	55
	3.5 Summary and Conclusions	55
4.0 Penetration Leakage Assessment		66
	4.1 Leak Rate Calculations for the Reactor Vessel Head Penetration	66
	4.2 Reactor Vessel Head Wastage Assessment/Comparison to ASME Code Allowables	85

TABLE OF CONTENTS (continued)

Section		Page
5.0	Plant/Penetration Categorization	93
	5.1 Plant Categorization	93
	5.2 Microstructure Characterization Studies	97
6.0	References	109

List of Figures

Figure	Title	Page
2-1	Three-Dimensional Model of the 4-Loop Outermost Penetration	4
2-2	Three-Dimensional Model of the 4-Loop Intermediate Penetration	5
2-3	Three-Dimensional Model of the 4-Loop Center Penetration	6
2-4	Steady State Operational Stresses for Outer Penetration	8
2-5	Stress Plots Along Inside Surface of Outer Penetration	10
2-6	Stress Distribution at Steady State Condition of Outer Penetration	11
2-7	Stress Plots Along Outside Surface of Outer Penetration	12
2-8	Stress Plots Along Inside Surface of Intermediate Penetration	14
2-9	Stress Distribution at Steady State Condition of Intermediate Penetration	15
2-10	Stress Plots Along Inside and Outside Surfaces of Center Penetration	16
2-11	Stress Distribution at Steady State Condition of Center Penetration	17
2-12	Model Mesh (Isoparametric-Axisymetric Model)	19
2-13	Current Boundary Conditions on R/V Head Penetration Models	20
2-14	Location of Line S6S3 in Model Mesh	22
2-15	Displaced Element Plot (Bolt-Up and Pressure Loadings)	23
2-16	Hoop Stress X-Y Plane σ_ρ (Bolt-Up Load Only)	24
2-17	Hoop Stress Z Direction σ_y (Bolt-Up Load Only)	24
2-18	Hoop Stress X-Y Plane σ_ρ (Pressure Load Only)	25
2-19	Hoop Stress Z Direction σ_y (Pressure Load Only)	25
2-20	Hoop Stress X-Y Plane σ_ρ (Bolt-Up and Pressure Load)	26
2-21	Hoop Stress Z Direction σ_y (Bolt-Up and Pressure Load)	26
2-22	Weld Length on Head Penetration Tube	29
2-23	Test Specimen	34
2-24	Head Penetration Tube Sample	34
2-25	Cyclic Stress-Strain loading Representation	36
2-26	Hold Time Stress-Strain Test Graphical Representation	36
2-27	Alloy 600 head Penetration Material	42
2-28	Alloy 600 Material	43
2-29	Alloy 600 Material Stress-Strain Curves	44
2-30	Estimated Fatigue Curves for Test Material and Actual Test Data for Special Tests	45
2-31	Maximum Hoop Stress as a Function of Penetration Angular Location	49
3-1	Crack Growth Rate Measurements in the 1200 ppm B, 2.2 ppm Li Baseline Environment	58
3-2	Crack Growth Rate Results for Statically and Actively Loaded Specimens in Three Different Environments	59
3-3	Scotts Model for SCC Growth Rates in Alloy 600 in Primary Water Environments (330°C)	60

List of Figures (continued)

Figure	Title	Page
3-4	Validation of Crack Growth Law with Field Data	61
3-5	Summary of Temperature Effects on SCC Growth Rates for Alloy 600 in Primary Water, Laboratory and Field Experience	62
3-6	Crack Growth Predictions for Surface Flaws Below and At the Weld Region in the Head Penetrations for a Range of Temperatures	63
3-7	Crack Growth Predictions for Through-Wall Flaws Located Below the Weld in Head Penetrations for a Range of Temperatures	64
3-8	Crack Growth Predictions for Growth At and Below the Weld on the Upper Hillside Location, for a Range of Temperatures	65
4-1	Head Penetration and Vessel Assembly	80
4-2	Leak Rate as a Function of Clearance and Crack Lengths in Terms of Liters per Minute at the Exit of Annulus Clearance Between Head Penetration and Vessel	81
4-3	Leak Rate as a Function of Clearance and Crack Lengths in Terms of GPM at the Exit of Annulus Clearance Between Head Penetration and Vessel	82
4-4	Predicted Leak Rate for Hydrotest Conditions - Short Cracks	83
4-5	Predicted Leak Rate for Hydrotest Conditions - Large Cracks	84
4-6	WOG Plant Reactor Vessel Head Penetration Leakage - Postulated Wastage Defect Geometries	91
4-7	Reactor Vessel Head Wastage Analysis Model for Four Loop Head	92
5-1	Knoop Hardness Traverses on the Transverse Cross-Section of a Jamesport Penetration Tube Wall Starting at a Ground Surface and at a Machined Surface	100
5-2	SEM Micrographs Illustrating the Microstructure of the Alloy 600 Sample Obtained from the Beaver Valley Station Penetration Tube Calibration Standard (Bromine etch)	101
5-3	SEM Micrographs Illustrating the Microstructure of the Alloy 600 Sample Obtained from the Vogtle Station Penetration Tube Calibration Standard (Bromine etch)	102
5-4	SEM Micrographs Illustrating the Microstructure of the Alloy 600 Sample Obtained from the St. Lucie Station Penetration Tube Calibration Standard (Bromine etch)	103
5-5	SEM Micrographs Illustrating the Microstructure of the Alloy 600 Penetration Tube Found in the Jamesport Unit 1 Reactor Vessel Closure Head (Bromine etch)	104
5-6	SEM Micrographs Illustrating the Microstructure of the Alloy 600 Sample Obtained from the Braidwood Station Penetration Tube Calibration Standard (Bromine etch)	105

List of Figures (continued)

Figure	Title	Page
5-7	SEM Micrographs Illustrating the Microstructure from a Spare Piece of the Alloy 600 Material Heat Used in the Ringnals Unit 3 Reactor Vessel Head Penetration Tubes (Bromine etch)	106
5-8	SEM Micrographs Illustrating the Microstructure of the Alloy 600 Sample Obtained from the Byron Station Penetration Tube Calibration Standard (Bromine etch)	107
5-9	SEM Micrographs Illustrating the Microstructure of the Alloy 600 Sample Obtained from the Watts Bar Station Penetration Tube Calibration Standard (Bromine etch)	108

List of Tables

Table	Title	Page
2-1	Hoop Stress Summary at Node 297	27
2-2	CRDM Weld Adapter Partial Penetration Weld Lengths	30
2-3	Cyclic Stress-Strain Test Results	38
2-4	Results for the 10 Block Cyclic Test, Specimen Number 65-03	38
2-5	Results for the [ ]^c Block Test Specimen Number 65-04	39
2-6	Hold Time Stress-Strain Test Results	40
2-7	Modulus of Elasticity (E) for Test Specimens	41
2-8	Comparison of Vessel Sizes	46
2-9	Results of 2-D Center Model at Steady State, Effect of Vessel Size	47
2-10	Maximum Hoop Stresses Along Inside Surfaces at Steady State - 4 Loop Plant	48
2-11	Maximum Hoop Stress Calculation for 2 & 3 Loop Plants	48
2-12	Summary of 4-loop Penetration Steady State Stress	51
3-1	Temperature Correction Factors for Crack Growth: Alloy 600	57
4-1	Leak Rates Through a Range of Crack Lengths: Head Penetration	73
4-2	Crack Length, Mass Flux and heat Capacity Ration in the Annulus Clearance between Penetration and Vessel	74
4-3	Leak Rate Through the Annular Clearance between the Heat Penetration and Vessel	75
4-4	Final Leak Rate at the Exit of Annulus Clearance Between Head Penetration and Vessel	76
4-5	Final Leak Rate Calculation for Penetration with Reported Leak	78
4-6	Summary of Wastage Evaluation Stress Analysis	90
5-1	Summary of Metallography Results on Alloy 600 Penetration Tube Materials	99

Executive Summary

An extensive evaluation has been carried out to characterize the loading and stresses which exist in the head penetrations of Westinghouse plants. Three-dimensional finite element models were constructed, and all known loadings on the penetrations were analyzed. These loadings included internal pressure, thermal expansion, and interference fits, as appropriate. In addition, residual stresses due to the welding of the penetrations to the vessel head (as evidenced by the observed ovality) were considered, using an elastic-plastic finite element analysis.

Results of the analyses reported here are consistent with the axial orientation and location of flaws which have been found in service in a number of plants, in that the largest stress component is the hoop stress, and the peak stresses were found to exist in the penetrations whose circumferential locations are farthest away from the center of the vessel. The most important loading conditions were found to be those which exist on the penetration for the majority of the time, which are the residual stresses. These stresses are important because the reported cracking which has been observed to date in operating plants has been determined to result from primary water stress corrosion cracking (PWSCC), and were used in fracture calculations to predict the expected growth of flaws postulated to exist in the head penetrations. Crack growth laws were developed specifically for the range of operating temperatures of the head for Westinghouse plants, based on information from the literature as well as a compilation of crack growth data for operating plants.

Crack growth predictions show that the future growth of cracks which might be found in the penetrations will in general be very slow, in that, a number of years are expected for any significant extensions.

The safety consequences of an indication, below the weld, even if the indication were to have propagated through the penetration wall, would be of no consequence at all since the pressure boundary would not be broken unless the indication were to propagate above the weld.

The hoop stresses in the penetration remain larger than the axial stresses along the entire penetration. As such, further propagation of the indication would not change its orientation. Therefore, it is extremely unlikely that the head penetration would be severed as a result of any indications.

Any indication is unlikely to propagate very far up the penetration above the weld because the hoop stresses decrease in this direction. This decrease in hoop stress will cause the rate of propagation to slow down, and perhaps even to stop before the indication reaches the outside surface of the reactor vessel head. This result from the stress analysis supports the conclusion that it is extremely unlikely that leakage of any magnitude will occur.

For flaws above the vessel to penetration tube weld that propagate through wall, resulting in small leaks, corrosion/wastage of the low alloy carbon steel vessel head could occur. The potential

corrosion/wastage of the vessel head has been shown to be such that structural margins would be maintained within ASME Code allowables for six years of plant operation at 100% power.

The high likelihood that the indication will not propagate beyond the outer surface of the vessel head ensures that no catastrophic failure of the head penetration will occur. This is because the indication is expected to be enveloped in the head itself, which precludes the opening of the crack and limits leakage. In order to produce a failure of the head penetration, the flaw would have to extend over 13 inches above the head, which has been shown to be an extremely unlikely event. If crack growth beyond the outside surface of the reactor vessel head is considered, leakage will be detected prior to the crack reaching the critical flaw size of 13 inches above the vessel head. In fact, a through wall crack extending 2-3 inches above the penetration weld will allow leakage in excess of the 1.0 gpm Tech. Spec. limit for leakage from an unknown source and therefore would be detected long before the critical flaw size was reached.

1.0 INTRODUCTION

Reactor vessel head adapter penetrations fabricated from Alloy 600 material have experienced cracking during operation on at least [ ][8] French plants [ ].[4] The root cause of cracking in these French vessels' penetrations has been identified as primary water stress corrosion cracking (PWSCC) and has been reported to the WOG in Reference [ ] Domestic U.S. PWRs have penetrations of similar design as these French vessels although the service and material conditions typically represent appreciable differences between the French and domestic units.

In order to establish if potential cracking represents a possible safety condition the [ ] established a program to evaluate the various consequences of cracking. The components of this program include:

- Elastic/Plastic Analyses which envelop all Westinghouse Reactor Vessel Closure Head Penetrations.
- Crack Propagation Analysis
- Leakage Assessment
- Wastage Assessment of Low Alloy Steel Vessel Head

The program had three additional goals, not strictly related to the safety aspects of the penetration; (1) Establish a methodology for performing a relative ranking of an individual plant's susceptibility to PWSCC, (2) perform an assessment of typical Alloy 600 material microstructures used in the penetration tubes, and (3) perform an availability review/survey of "Low Leakage" detection systems.

2.0 PENETRATION STRESS ANALYSIS

2.1 Background

Several 3D-elastic finite element analyses performed previously to establish penetration stress magnitude and distribution, demonstrated that stresses caused by operational pressure and temperature [ ]^{b,c} loads are not large enough to cause penetration tube ovality of the magnitude which has been measured in a number of plants. Ovality measurements were based on penetration ID diametral and profile measurements taken from vessels of operating plants as well as plants which have not operated. It was further determined, qualitatively, that the residual stresses in and near the weld region due to welding are significantly higher than those caused by operational loads. Stresses experienced due to the welding fabrication processes used in attaching the penetration tube to the vessel head, exceed the yield strength of the Alloy 600 weld and penetration material. Therefore it became essential to perform additional stress analyses considering the inelastic mechanical properties of the penetrations, to more quantitatively define the stress field in the penetration.

2.2 Approach

The additional analyses not only have to be detailed enough to provide quantitative stress distributions, but also are needed to envelop all WOG plant penetrations. The 4-loop penetration geometries were judged to be enveloping. To help confirm that the analyses results of the 4-loop plant vessel head and penetrations were enveloping, a parametric study was performed to study the effect of a) vessel size and b) penetration location. The results indicated that the outermost penetrations of the 4-loop plant, which has the largest weld-offset angle among the 2, 3 and 4 loop plants, are the highest stressed penetrations under operating loads and have the largest residual stresses. Therefore, it was judged, using the elastic analysis and parametric study, that the outermost penetrations of the 4-loop plants are the enveloping penetrations of all WOG plants.

Having determined that the 4-loop plants envelope all WOG plants, three penetration models were built using temperature dependent elastic-plastic material properties. Three different penetration locations were modeled, they are:

1. The center location (#0)

2. The outermost location (e.g., penetration #78), and

3. A location between the outermost and center location (e.g., penetration #65)

In the Westinghouse 4-loop plant, penetrations #65 and #78 are located radially from the vessel centerline, [ ]^{b,c} inches respectively.

The models utilized finite element 3-dimensional isoparametric brick and wedge elements with one mid-side node on each side of the elements. Taking advantage of symmetry through the vessel and penetration centerlines only half the penetration geometry plus the surrounding vessel were modeled for penetrations 65 and 78. In the center penetration case it was necessary to model only one-quarter of the penetration as opposed to one-half the penetration. The difference being that for the center penetration there was not differential height across the weld (i.e., weld offset = 0.0 inch).

In all models the lower portion of the Control Rod Drive Mechanism (CRDM) Adapter tube (i.e., penetration tube), the adjacent section of the vessel closure head, and the joining weld are modeled. The vessel to penetration tube weld was simulated with two layers of elements. These models are shown in Figures 2-1, 2-2 and 2-3. The penetration tube, weld metal and cladding were modeled as Alloy 600 and the vessel head shell as carbon steel. Elements with elastic-plastic capabilities were incorporated in the weld region and surrounding elements in both the penetration tube and vessel head shell. The stress-strain material properties of the elastic-plastic elements representing Alloy 600 were derived from test data extracted using an actual Alloy 600 penetration material sample taken from the outermost penetration of a non-irradiated plant. [

]^{b,c}

To simulate the stress history of the penetration tube a loading sequence experienced by the penetrations was applied to each of the three models described above. The stresses caused by each of the load cycles were stored and maintained in the model before the next load cycle was applied to simulate the effect of residual stress. This provides for the accumulation of plastic stresses.

2.3 Elastic-Plastic Analysis Procedure

The load cycles described in Section 2.2 above are listed below:

[

]^{a,c}

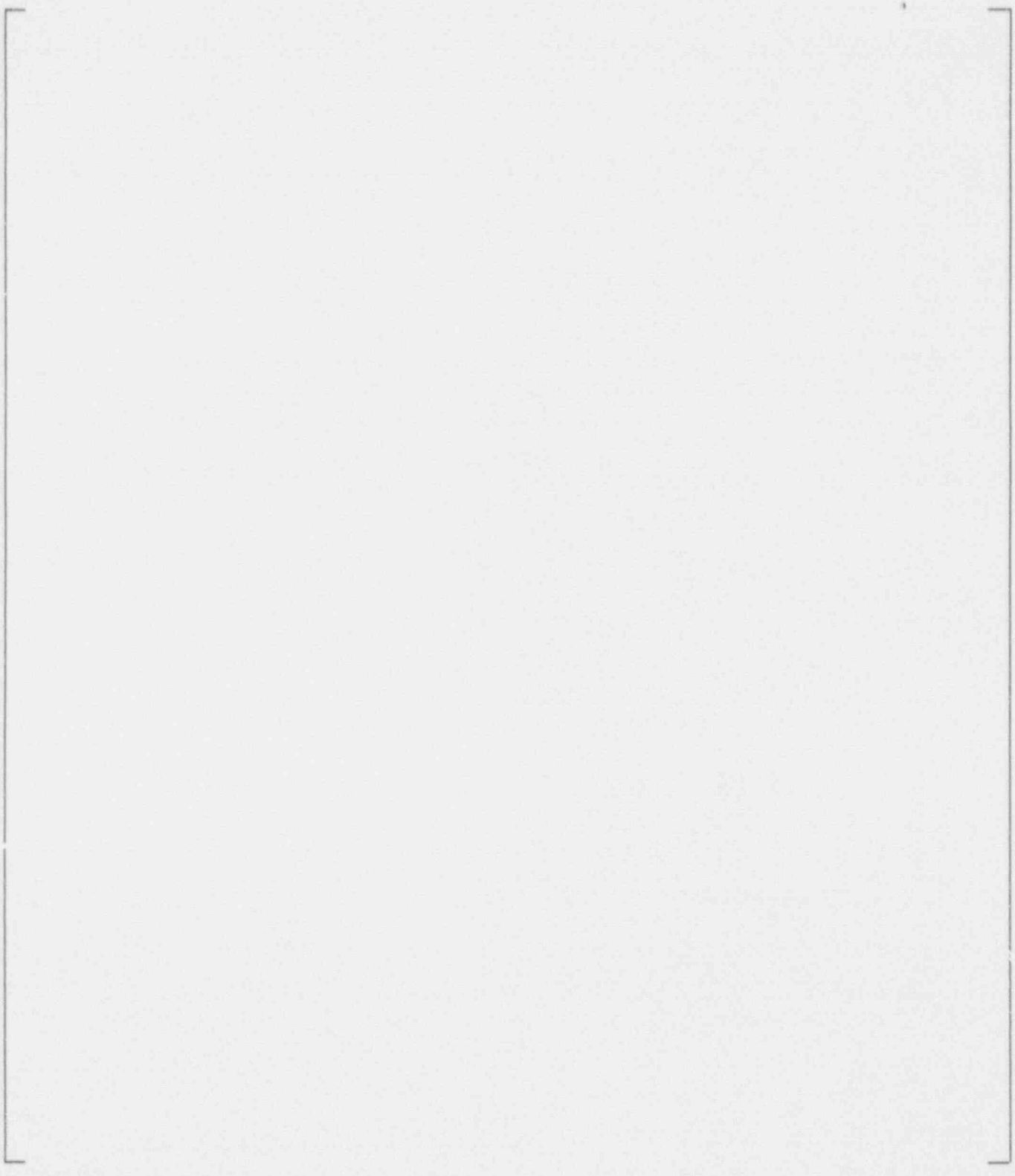

b,c

FIGURE 2-1
THREE-DIMENSIONAL MODEL OF THE 4-LOOP OUTERMOST PENETRATION

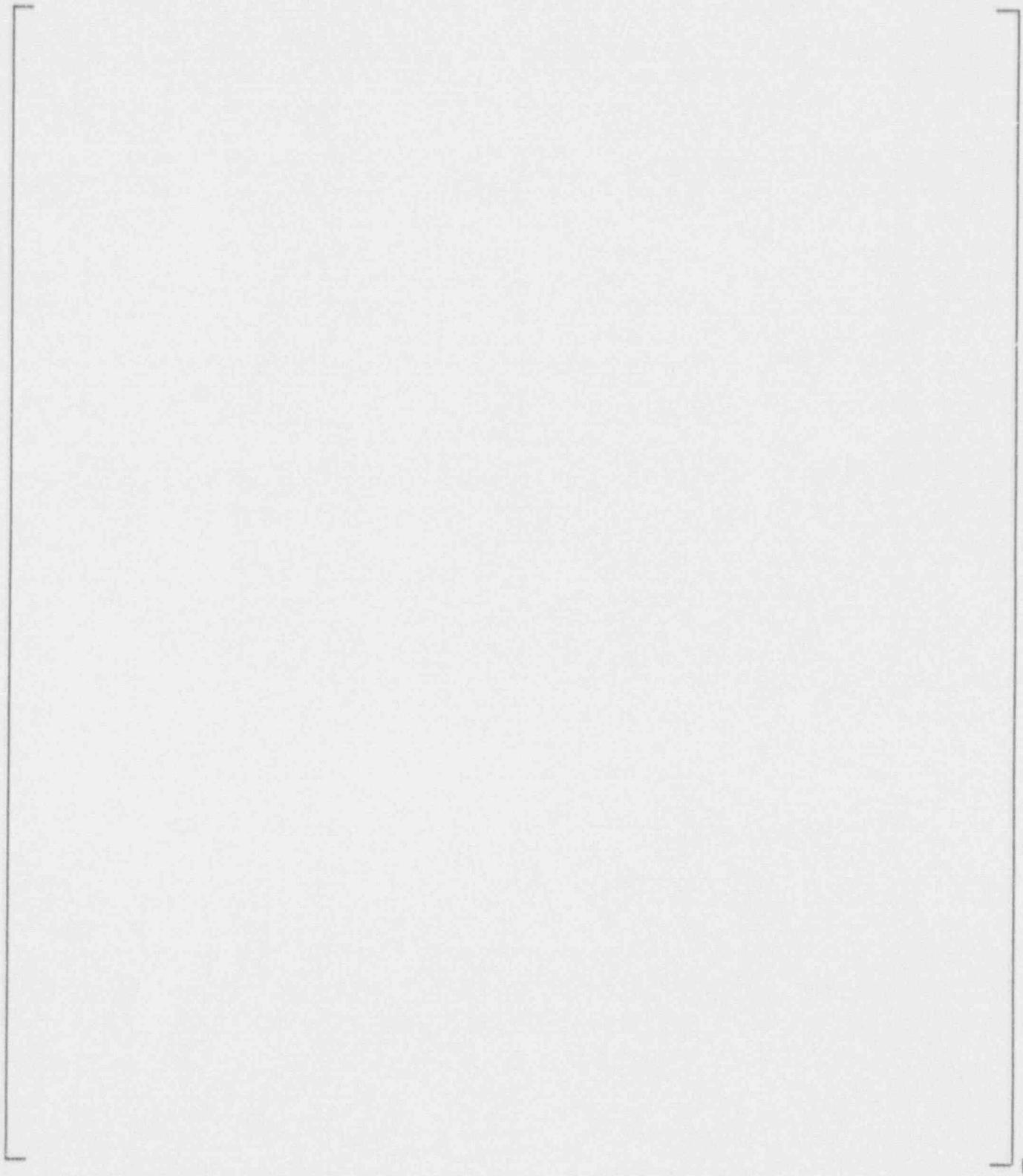

b,c

FIGURE 2-2
THREE-DIMENSIONAL MODEL OF THE 4-LOOP INTERMEDIATE PENETRATION

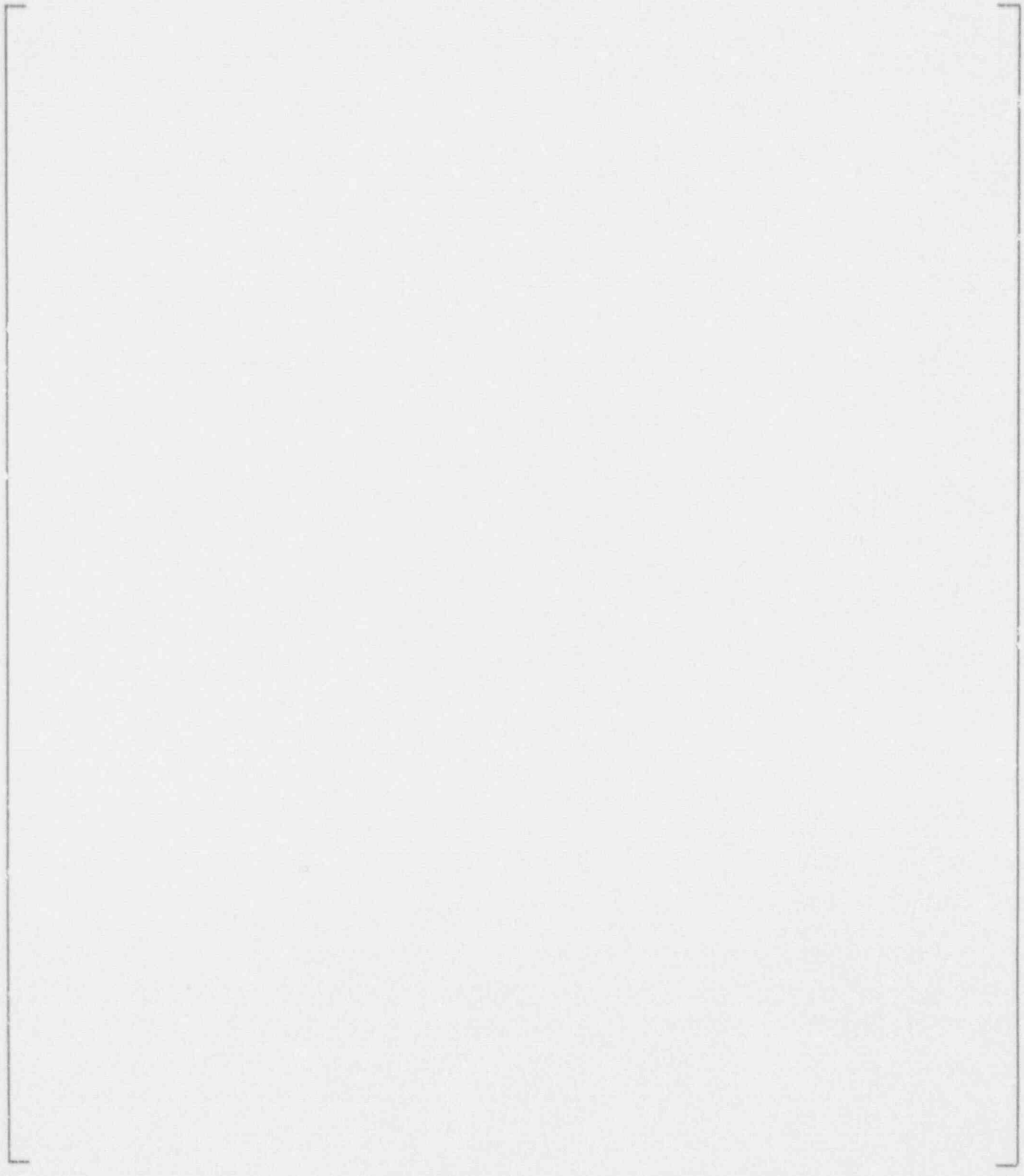

5),c

FIGURE 2-3
THREE-DIMENSIONAL MODEL OF THE 4-LOOP CENTER PENETRATION

it was found from the analysis that the welding process introduces significant residual stresses in the penetration tube near the partial penetration weld.

[ ] a,c

2.4 Stress Analysis Results – Outermost Penetration

The displacements of the vessel and penetration are shown in Figure 2-4 for steady state operation.

[ ] a,c

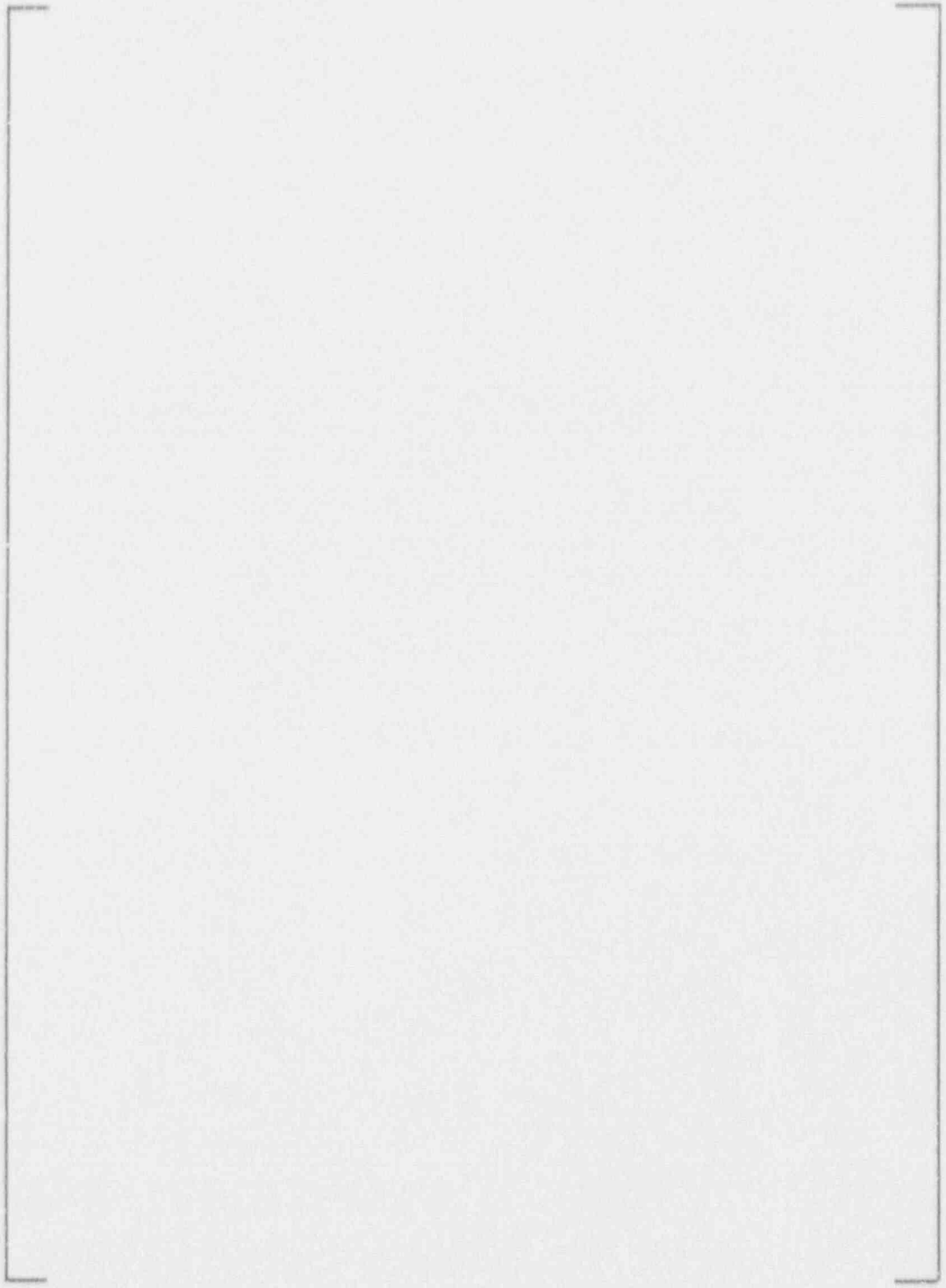

a,c

FIGURE 2-4
STEADY STATE DISPLACEMENT OF
R/V CLOSURE HEAD AND OUTERMOST PENETRATION

respect to Westinghouse supplied vessels, and was the maximum gap used in the leakage and wastage assessments.

The hoop, axial and effective (Von Mises) stresses for the steady state operating conditions on the inside surface along the peak stress lines are plotted in Figure 2-5. The highest stress lines along the inside diameter occur at two locations; a) along the side of the penetration nearest the center of the vessel (Line PA3), and b) the hillside which is furthest away from the center (180° away) (Line PA2). Note that these two locations correspond to the locations where axial cracks have been reported to exist.

[ ]a,c

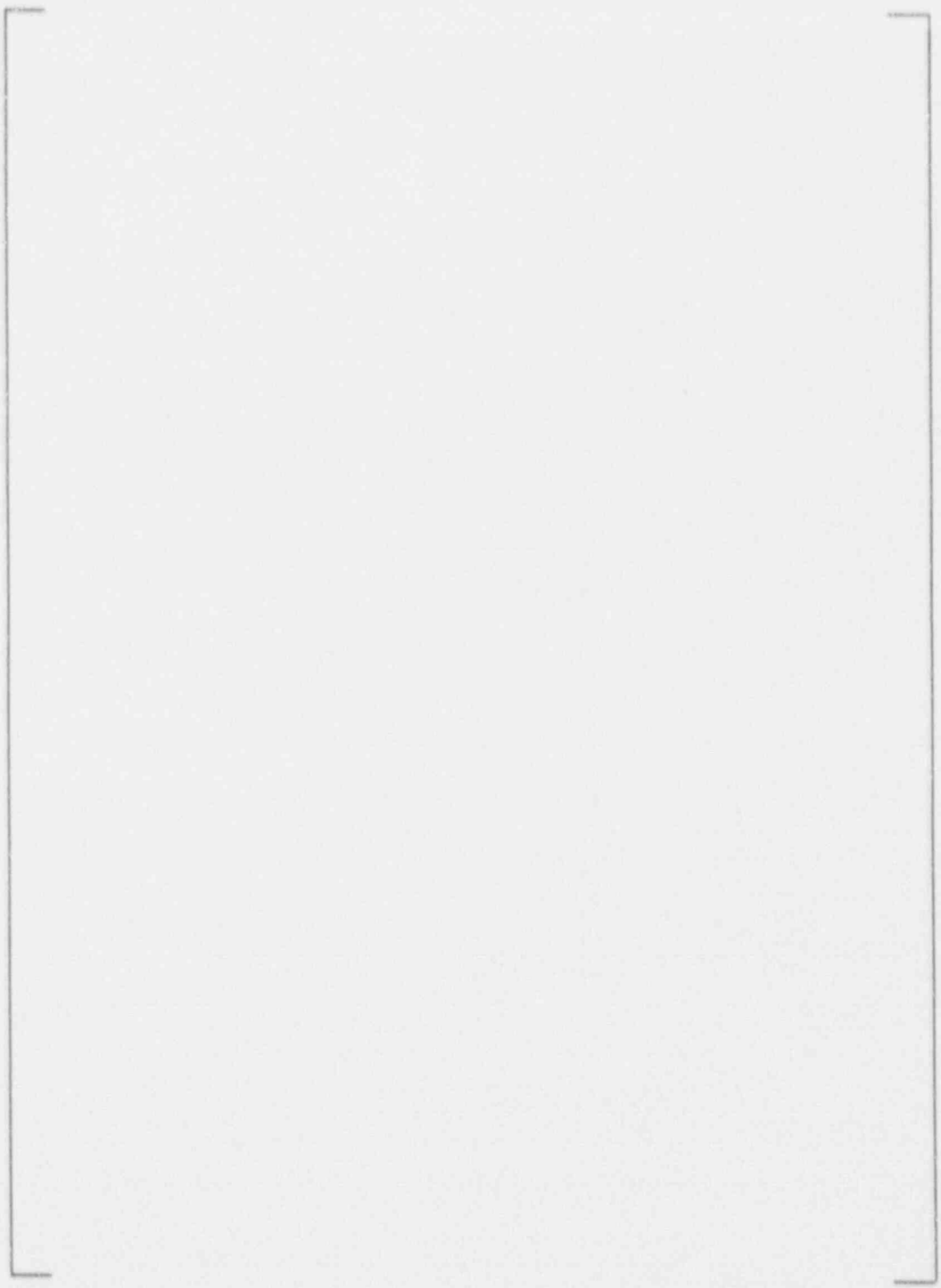

b,c

FIGURE 2-5
STRESS PLOTS ALONG INSIDE SURFACE
OF OUTER PENETRATION

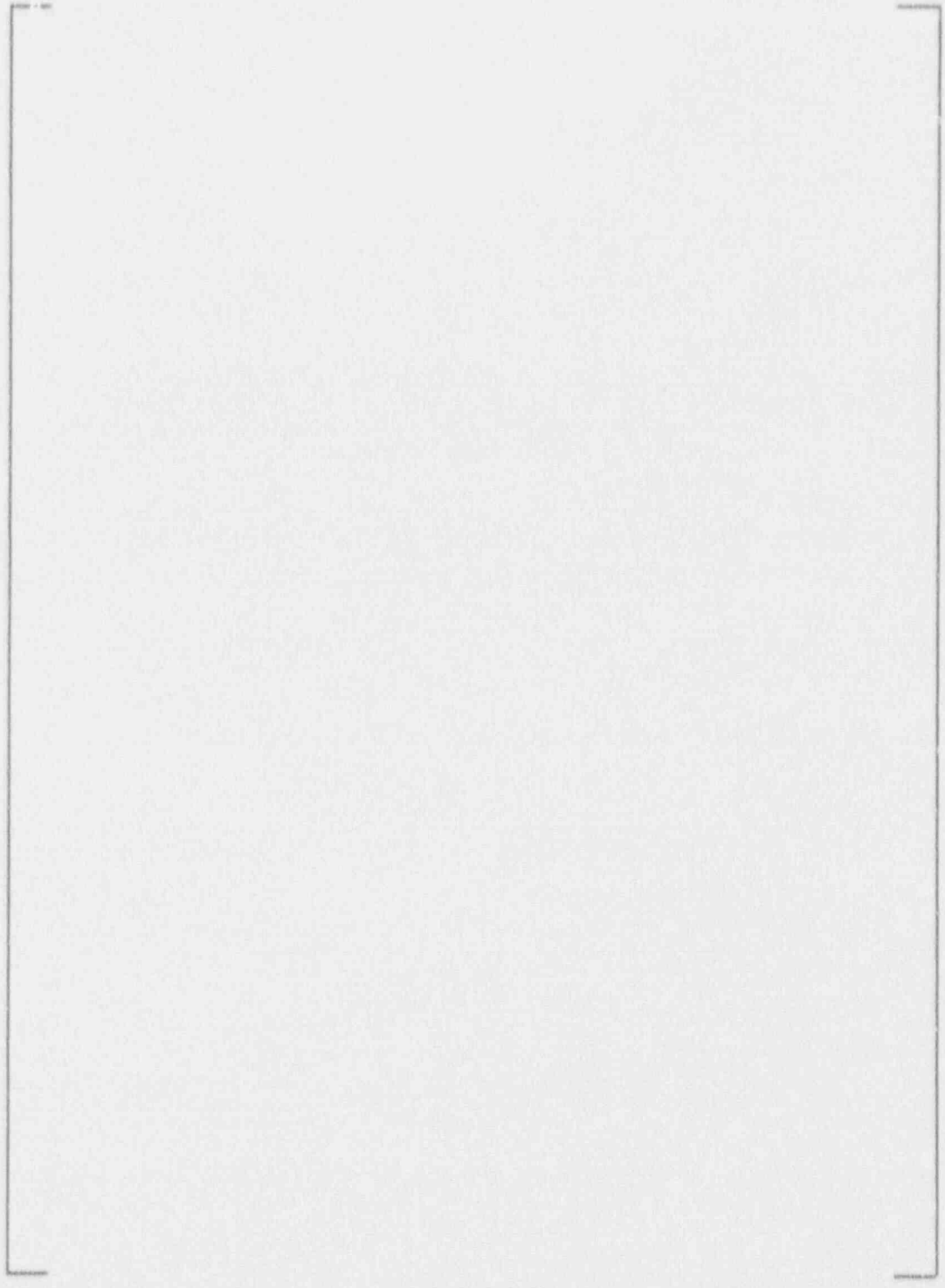

b,c

FIGURE 2-6
STRESS DISTRIBUTION AT STEADY STATE CONDITION
OF OUTER PENETRATION

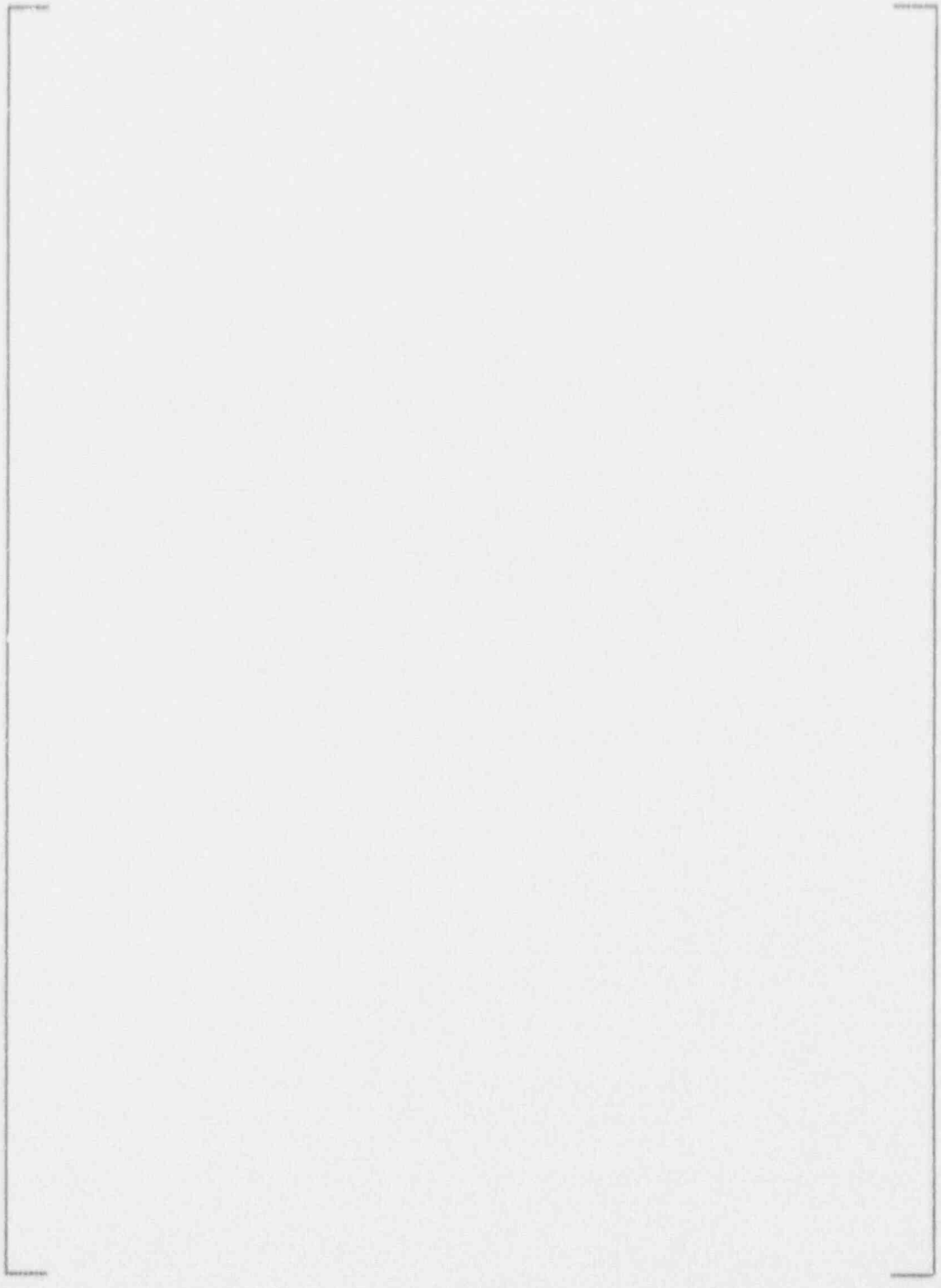

b,c

FIGURE 2-7
STRESS PLOTS ALONG OUTSIDE SURFACE
OF OUTER PENETRATION

2.5 Stress Analysis Results – Intermediate Penetration

The intermediate penetration analyzed is on a radius of [ ]^{b} from the vessel centerline (i.e., penetration no. 65 of a four loop plant). The stress analyses were carried out in precisely the same manner as the outermost penetration.

Figure 2-8 provides plots of the hoop, axial, and Von Mises stresses for the steady state operating conditions on the inside surface of the intermediate penetration tube along the peak stress lines. The peak stress lines correspond to those lines described for the outmost penetration. Figure 2-9 provides the hoop and axial stress distributions for the intermediate penetration.

2.6 Stress Analysis Results – Center Penetration

a,c

[

] The overall stress magnitudes are lower than those of the outer penetrations. The stress plot and contours along the inside and outside surfaces are shown in Figure 2-10 and 2-11 respectively.

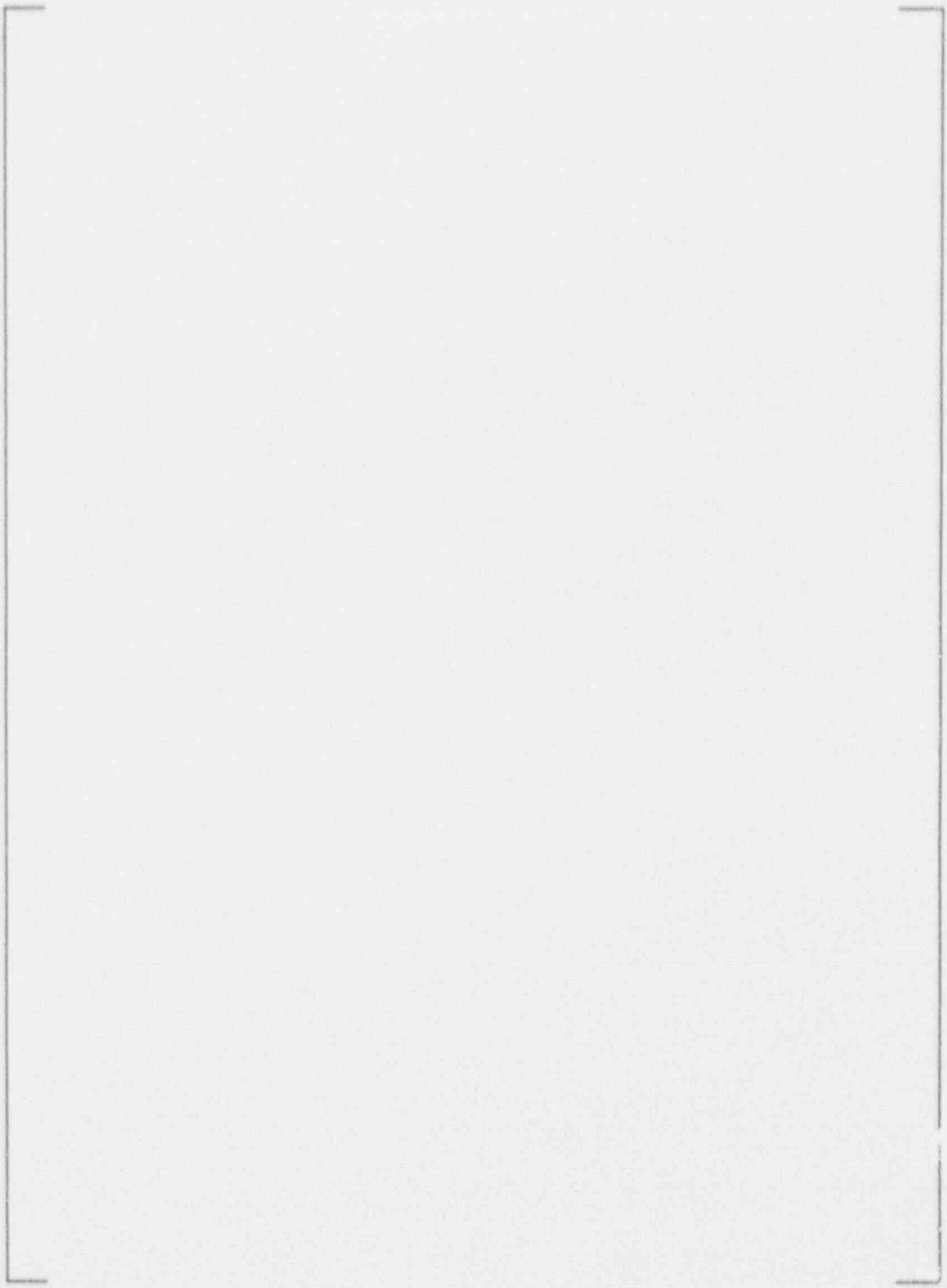

b,c

FIGURE 2-8
STRESS PLOTS ALONG INSIDE SURFACE
OF INTERMEDIATE PENETRATION

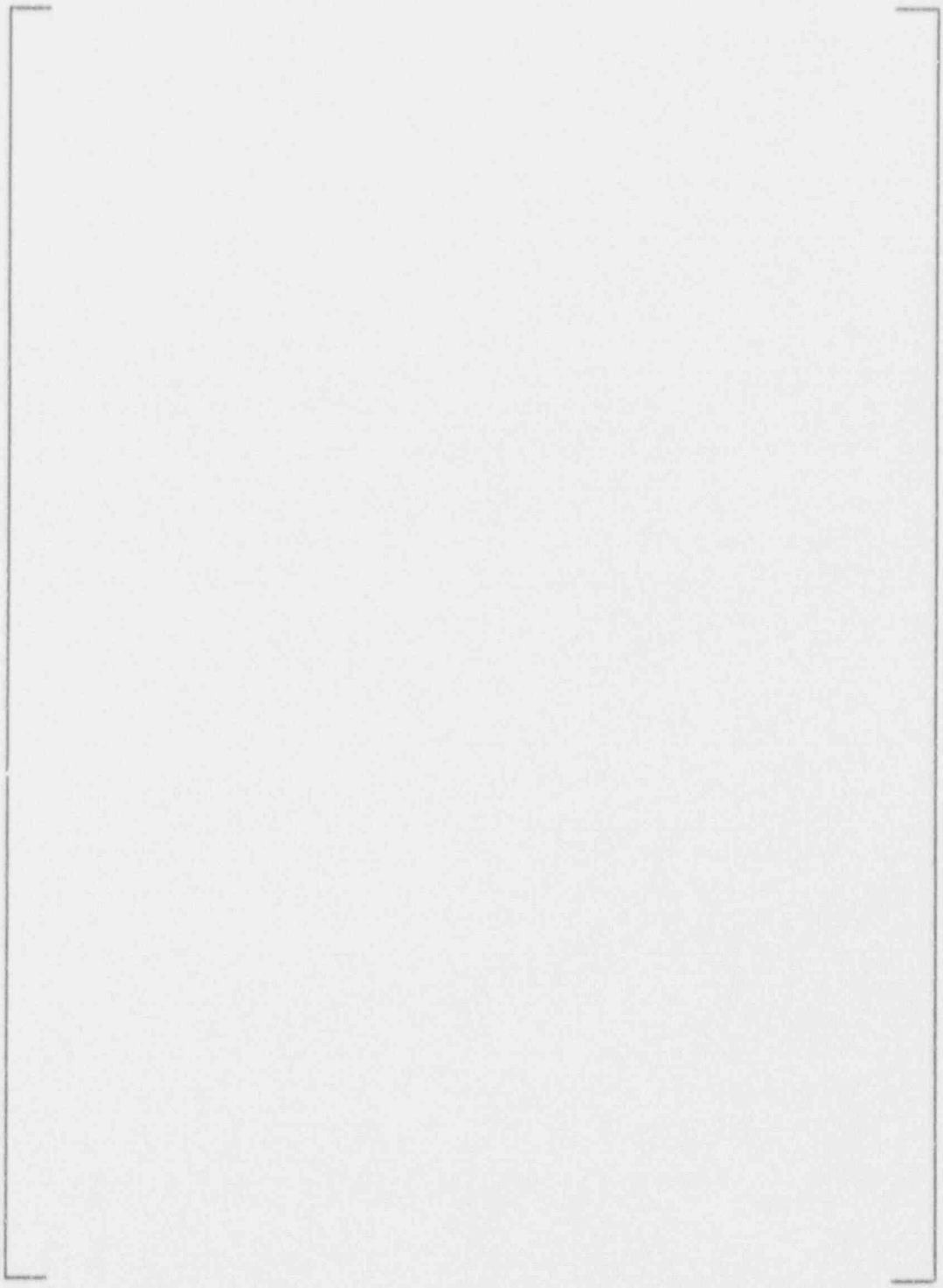

b,c

FIGURE 2-9
STRESS DISTRIBUTION AT STEADY STATE CONDITION
OF INTERMEDIATE PENETRATION

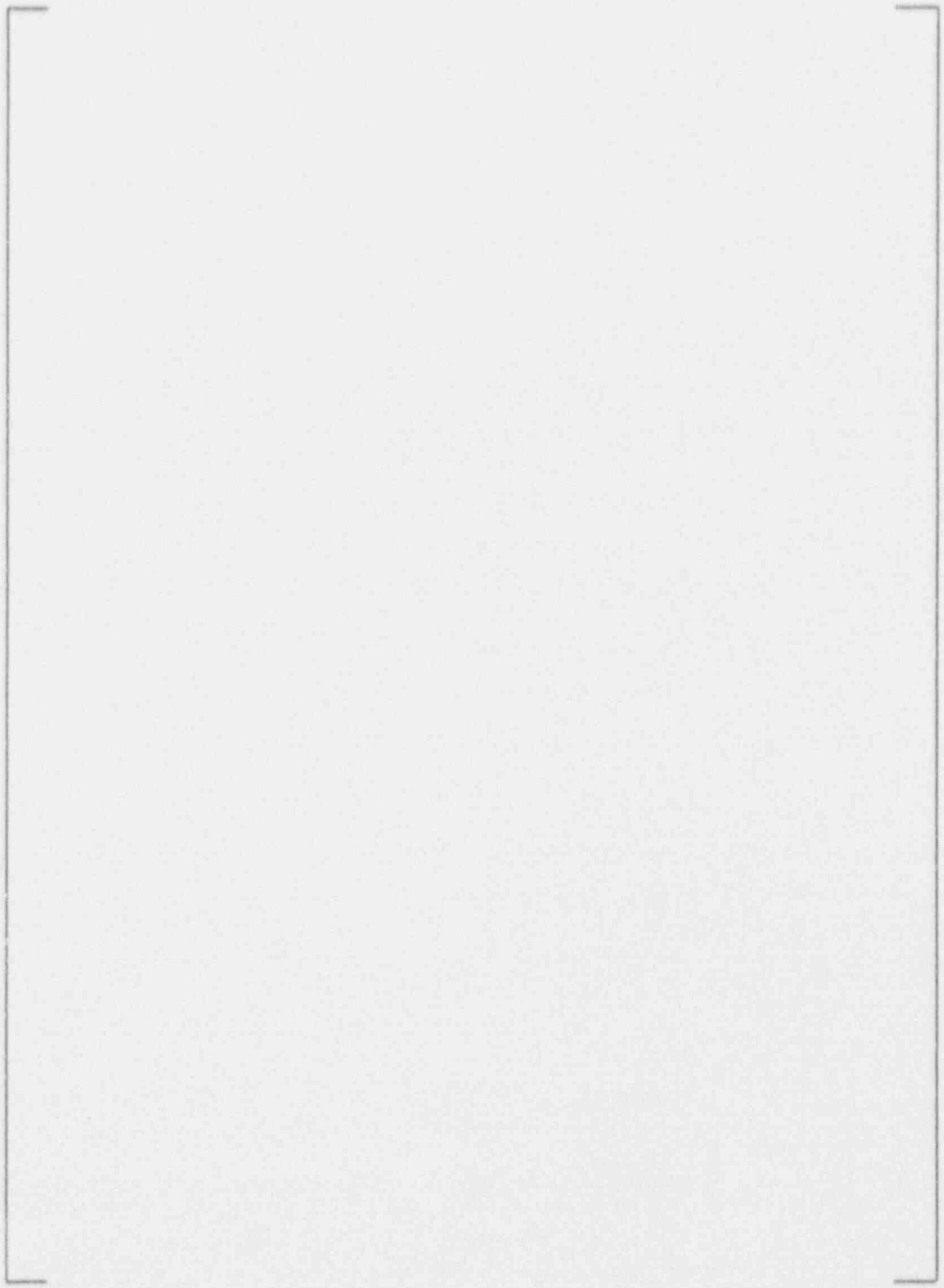

b,c

FIGURE 2-10
STRESS PLOTS ALONG INSIDE AND OUTSIDE SURFACES
OF CENTER PENETRATION

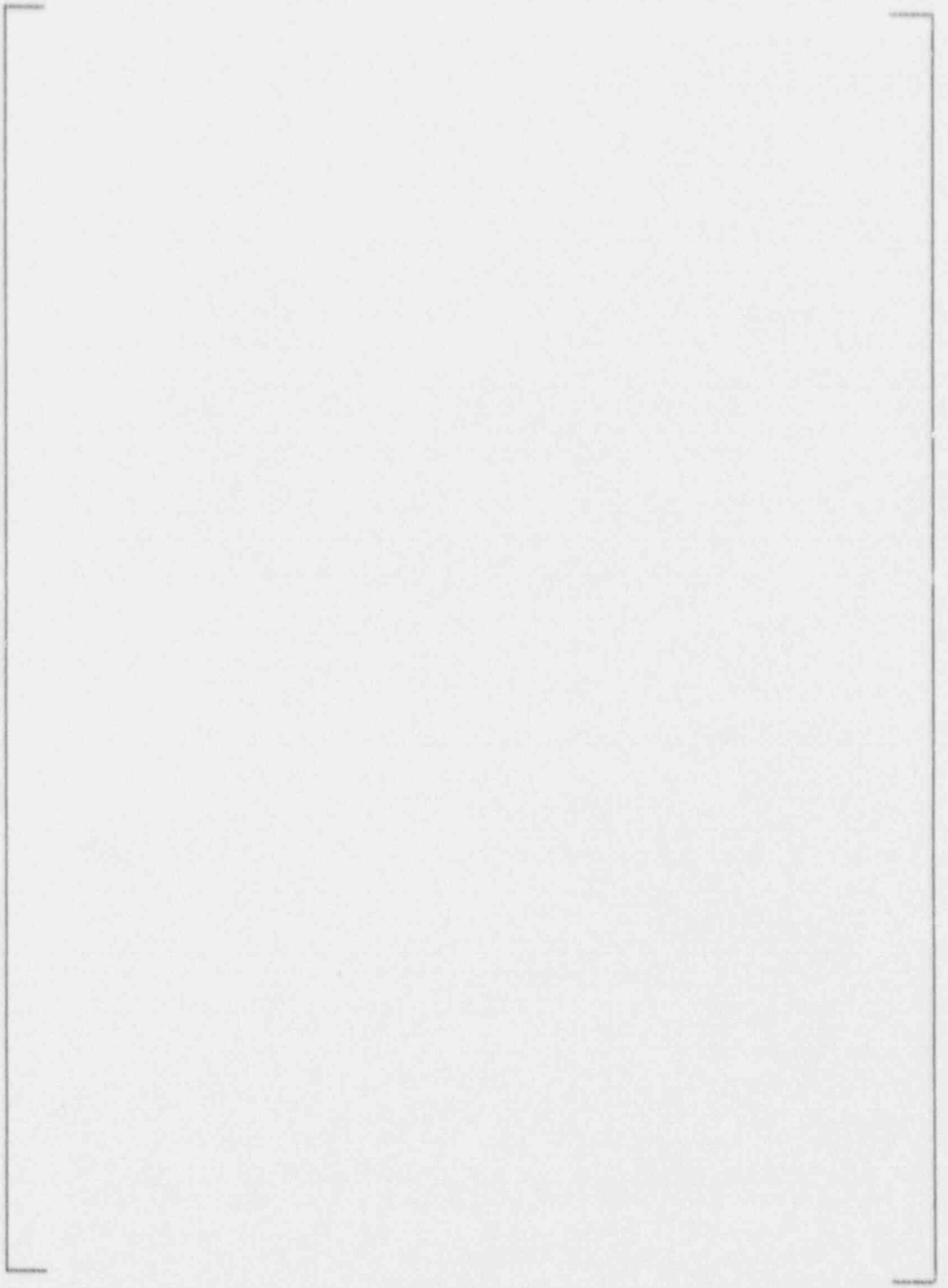

b,c

FIGURE 2-11
STRESS DISTRIBUTION AT STEADY STATE CONDITION
OF CENTER PENETRATION

2.7 Reactor Vessel Head Bolt-up Stress Contribution

An additional 2-dimensional, axisymmetric model was developed and used to determine the stress contribution in the closure head, due to bolt-up loads. Bolt-up loads are generated in the closure head by the rotation of the flanges caused by the tightening of the stud tensioners. The analysis evaluated the change in the stresses at a radial distance of 64.5 inches (penetration location #78) from the vessel centerline through the thickness of the shell. The conclusion of the analysis was that the bolt-up stresses are negligible compared to the operational stresses. This analysis also demonstrates that the simple boundary conditions (symmetry) used in the 3-dimensional, elastic-plastic analysis provide suitable constraints. A discussion of the analysis is included in the following paragraphs.

[ ] a,c

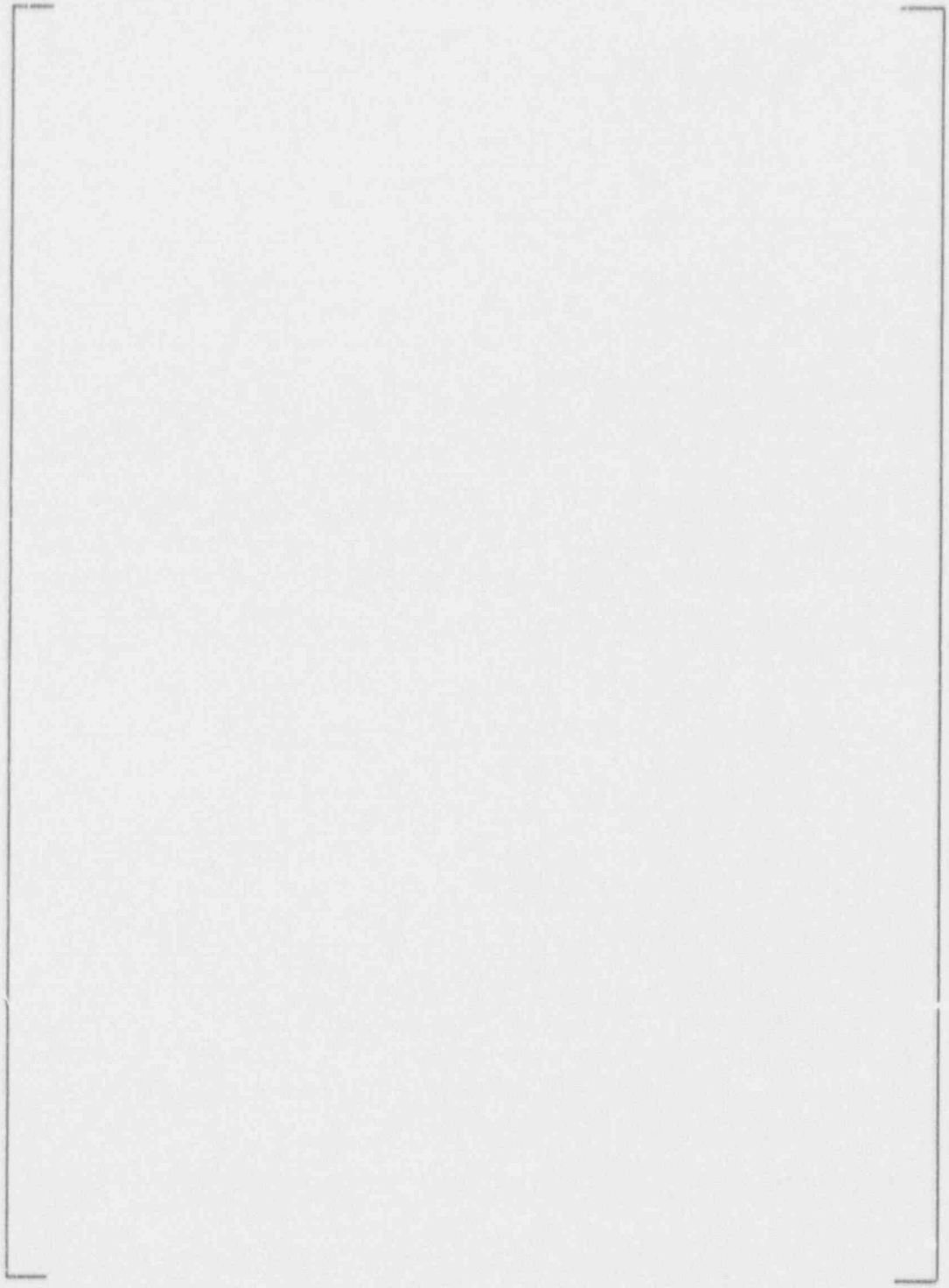

a,c

FIGURE 2-12
MODEL MESH (ISOPARAMETRIC-AXISYMMETRIC MODEL)

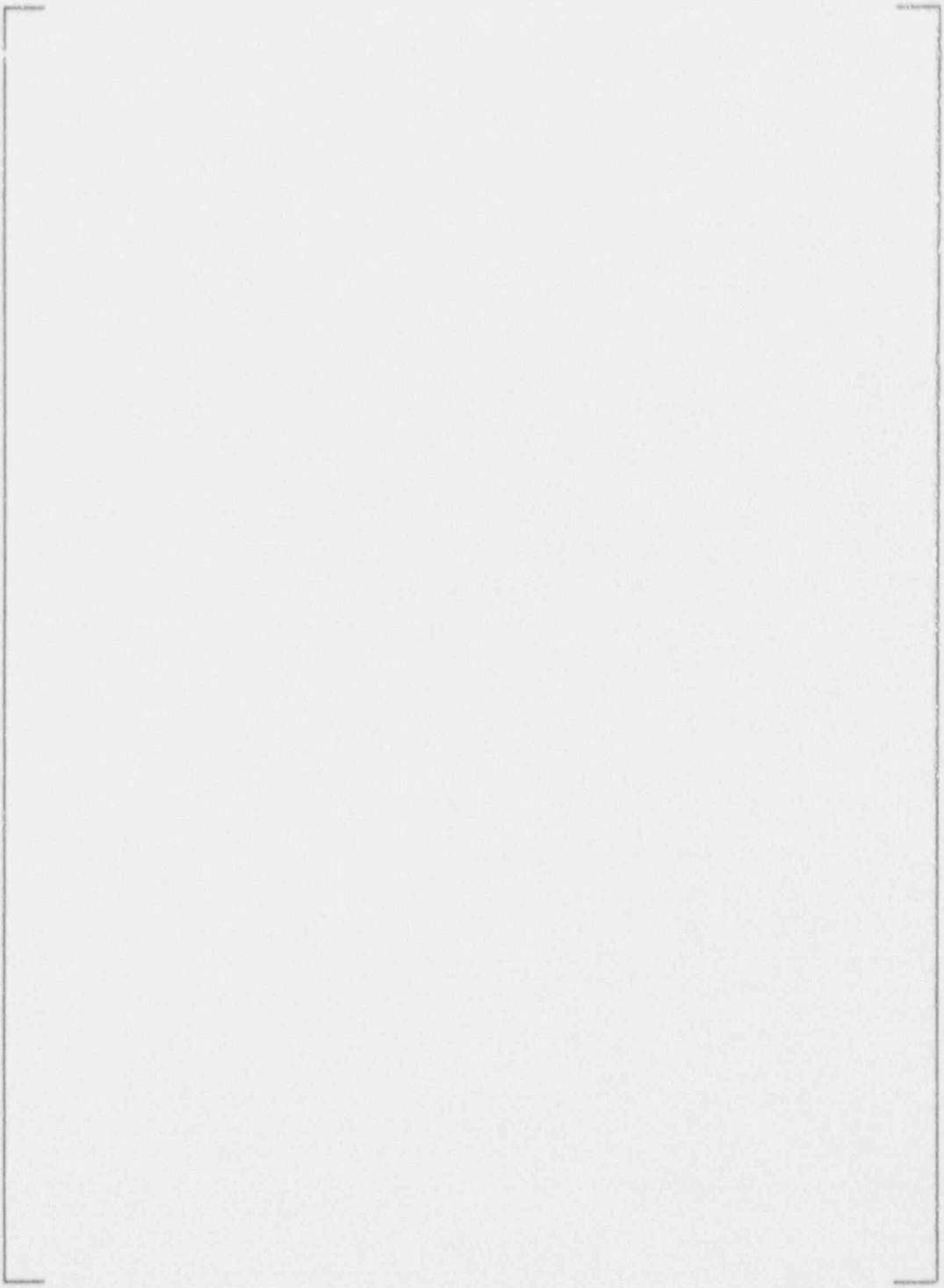

a,b,c

FIGURE 2-13
CURRENT BOUNDARY CONDITIONS ON R/V HEAD PENETRATION MODELS

The evaluation looked at the following three loads and load combinations:

1. Bolt-up Load Only (54 Studs @ 116.7 kips per stud).
2. Operating Pressure Only.
3. Bolt-up and Operating Pressure (2250 psi).

[ ] a,c

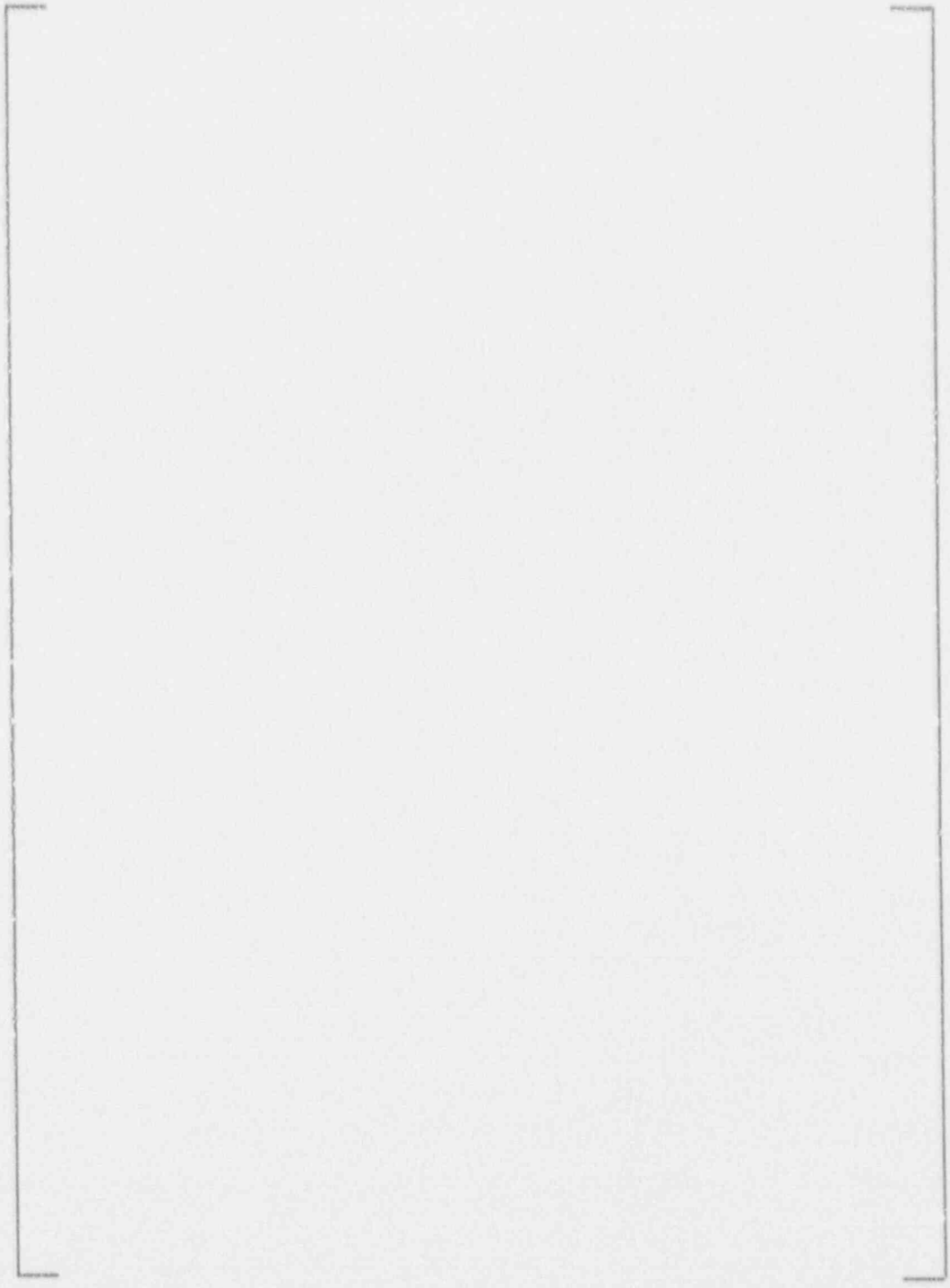

b,c

FIGURE 2-14
LOCATION OF LINE S6S3 IN THE MODEL MESH

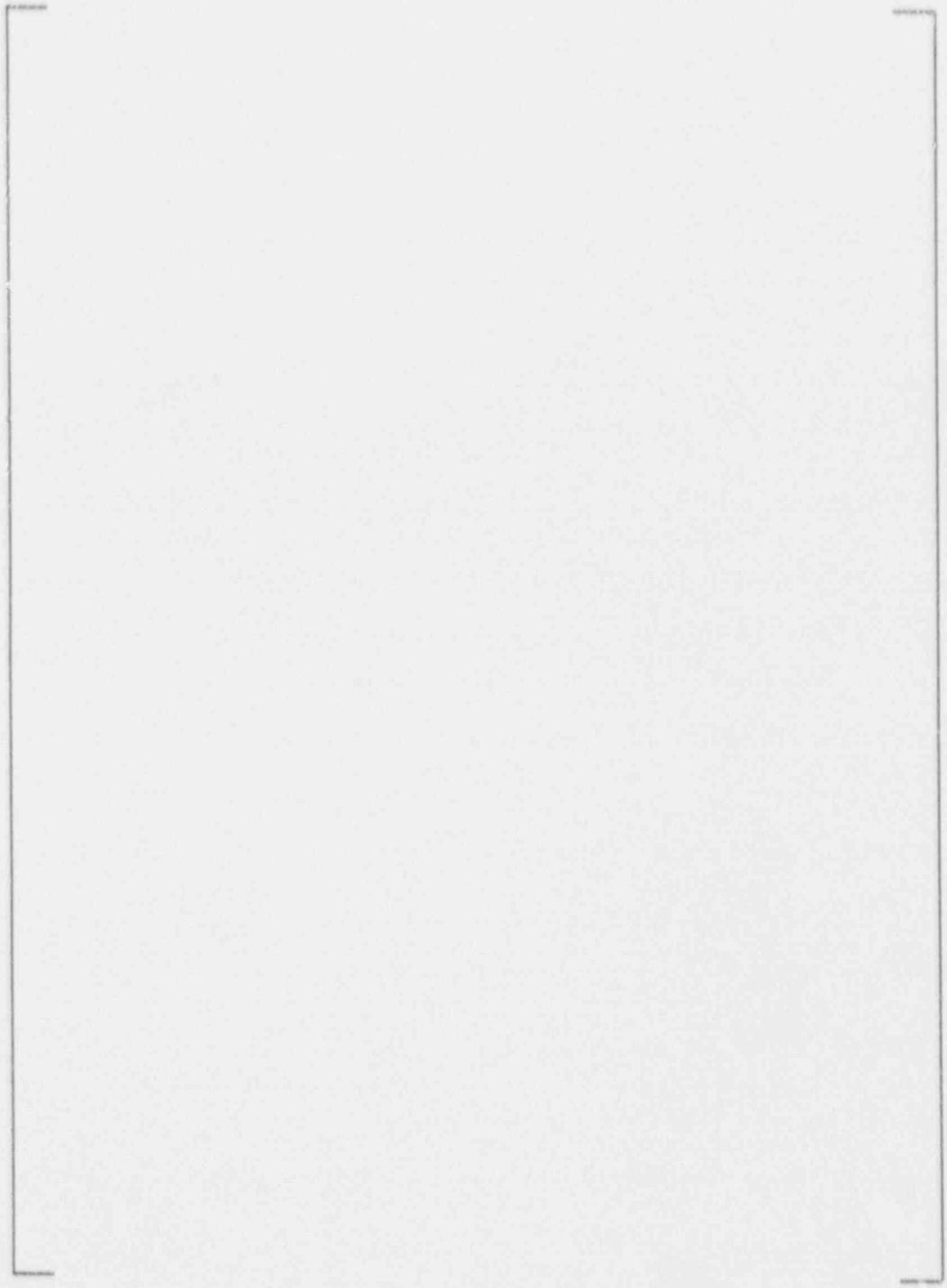

b,c

FIGURE 2-15
DISPLACED ELEMENT PLOT (BOLT-UP AND PRESSURE LOADINGS)

b,c

FIGURE 2-16
HOOP STRESS X-Y PLANE σ_ϕ (BOLT-UP LOAD ONLY)

b,c

FIGURE 2-17
HOOP STRESS Z DIRECTION σ_θ (BOLT-UP LOAD ONLY)

b,c

FIGURE 2-18
HOOP STRESS X-Y PLANE σ_ϕ (PRESSURE LOAD ONLY)

b,c

FIGURE 2-19
HOOP STRESS Z DIRECTION σ_θ (BOLT-UP LOAD ONLY)

b,c

FIGURE 2-20
HOOP STRESS X-Y PLANE σ_ϕ (BOLT-UP AND PRESSURE LOAD)

b,c

FIGURE 2-21
HOOP STRESS Z DIRECTION σ_θ (BOLT-UP AND PRESSURE LOAD)

Table 2-1 below summarizes the stresses calculated at node 297. [

]a,c

TABLE 2-1

[

]b,c

2.8 ASME Code/Reactor Vessel Head to Penetration Tube Weld Conservatism

The ASME B&PV Code has used the same criteria for setting the penetration tube partial penetration weld size since the original publication of Section III in 1963. This criteria is presented in Paragraph 4.57(c) of the 1963 edition and corresponding paragraphs of later editions. The corresponding Paragraph is NB 3337.3(a) in the 1989 edition of Section III, which is the latest version approved for use by the NRC. This criteria states that, "Partial penetration welds shall be of sufficient size to develop the full strength of the attachment (in 1963) or nozzles (in 1989)." This criteria is based on one of the basic tenets of the ASME B&PV Code, that all vessel pressure boundary welds must be as strong as the weakest of the two parts joined together. This criteria was established so that the weld was not the "weak-link" or weakest part in the assembly such that any potential failure would be expected to occur in the base metal, not the weld.

The vessel fabricators used varying degrees of margin or conservatism on the weld sizes specified on their fabrication drawings to comply with the ASME Code specified minimum dimensions for the penetration tube weld detail. These weld details are shown in Code Figures 462.4(d) in the 1963 code and corresponding figures through Figure NB 4244(d)-1 in the 1989 code. These figures have the same dimensions for the original or standard partial penetration design. However, there was an alternate design added to these figures starting with the 1969 summer addenda.

The maximum lengths of the penetration tube to reactor vessel head weld at the outermost CRDMs varied among vessel vendors. These variations were due to vessel vendor interpretations of the Code rules for the original weld design.

[ ]

a,c

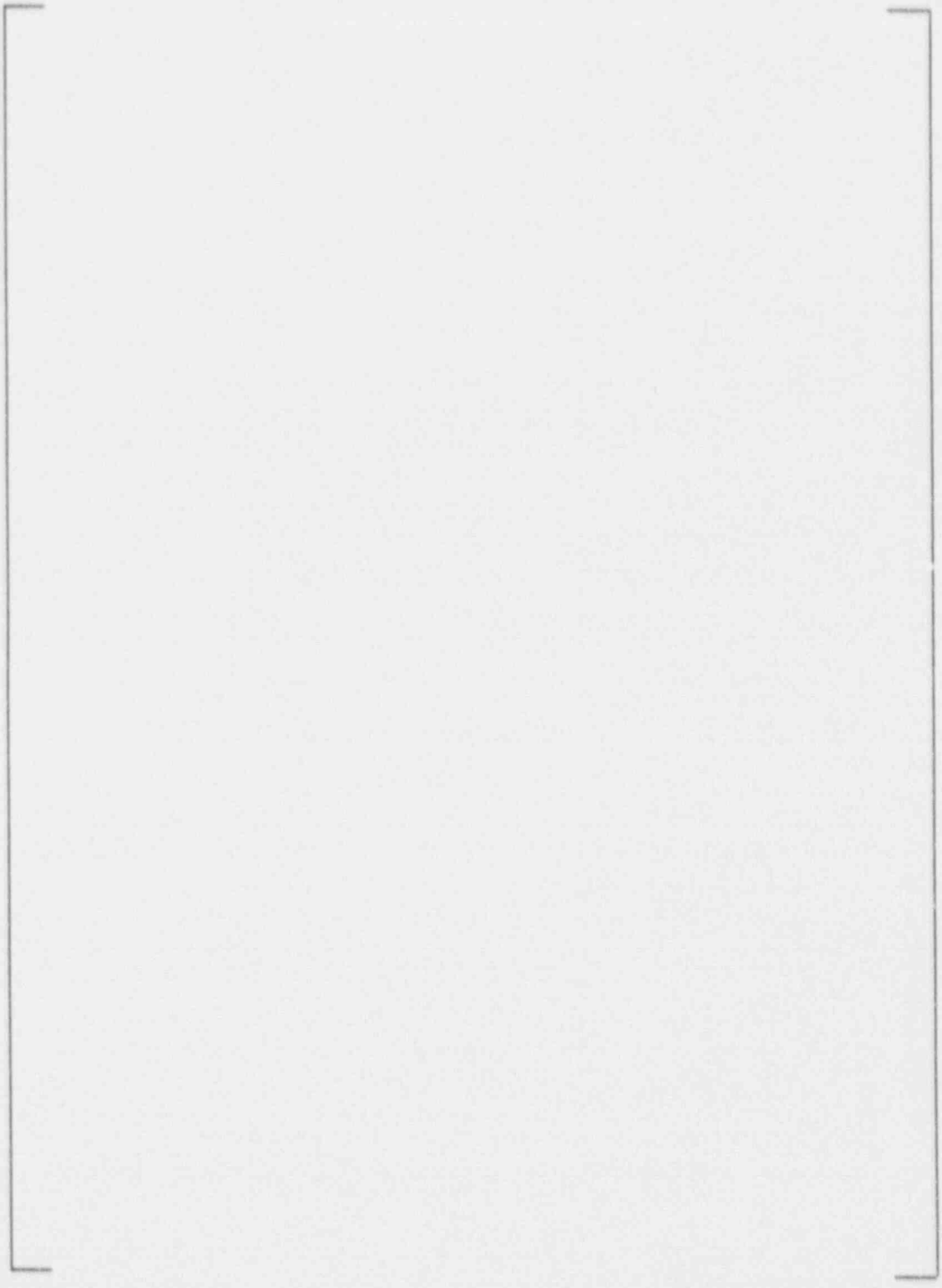

b,c

FIGURE 2-22
WELD LENGTH ON HEAD PENETRATION TUBE

Table 2-2

CRDM Weld Adapter Partial Penetration Weld Lengths

b,c

Table 2-2 (cont)

CRDM Weld Adapter Partial Penetration Weld Lengths

b,c

Table 2-2 (cont)

CRDM Weld Adapter Partial Penetration Weld Lengths

[ ]

b,c

2.9 Development of Stress/Strain Curves

Tests were performed to investigate the stress-strain relationship of Alloy 600 material for typical Westinghouse PWR reactor vessel head penetrations. These tests were performed to help determine the actual material characteristics and fatigue life of "as-installed" Alloy 600 head penetration material at 600°F.

2.9.1 Purpose

[

]

2.9.2 Method

[

]

2.9.3 Test Specimen

[

]

a,c

FIGURE 2-23
TEST SPECIMEN

a,c

FIGURE 2-24
HEAD PENETRATION TUBE SAMPLE

2.9.4 Test Description

[ ]

a,b,c

b,c

FIGURE 2-25
CYCLIC STRESS-STRAIN LOADING REPRESENTATION

b,c

FIGURE 2-26
HOLD TIME STRESS-STRAIN TEST GRAPHICAL REPRESENTATION

Step 1 (Cycle 1)

[ ]

a,b,c

2.9.5 Test Results

[ ]

a,b,c

Table 2-3

Cyclic Stress-Strain Test Results

[ ] b,c

Table 2-4

Results for the 10 Block
Cyclic Test, Specimen Number 65-03

[ ] b,c

Table 2-5

Results for the [ ]^{c} Block Test,
Specimen Number 65-04

[ ] a,b,c

Table 2-6

Hold Time Stress-Strain Test Results

a,b,c

[

a,b,c]

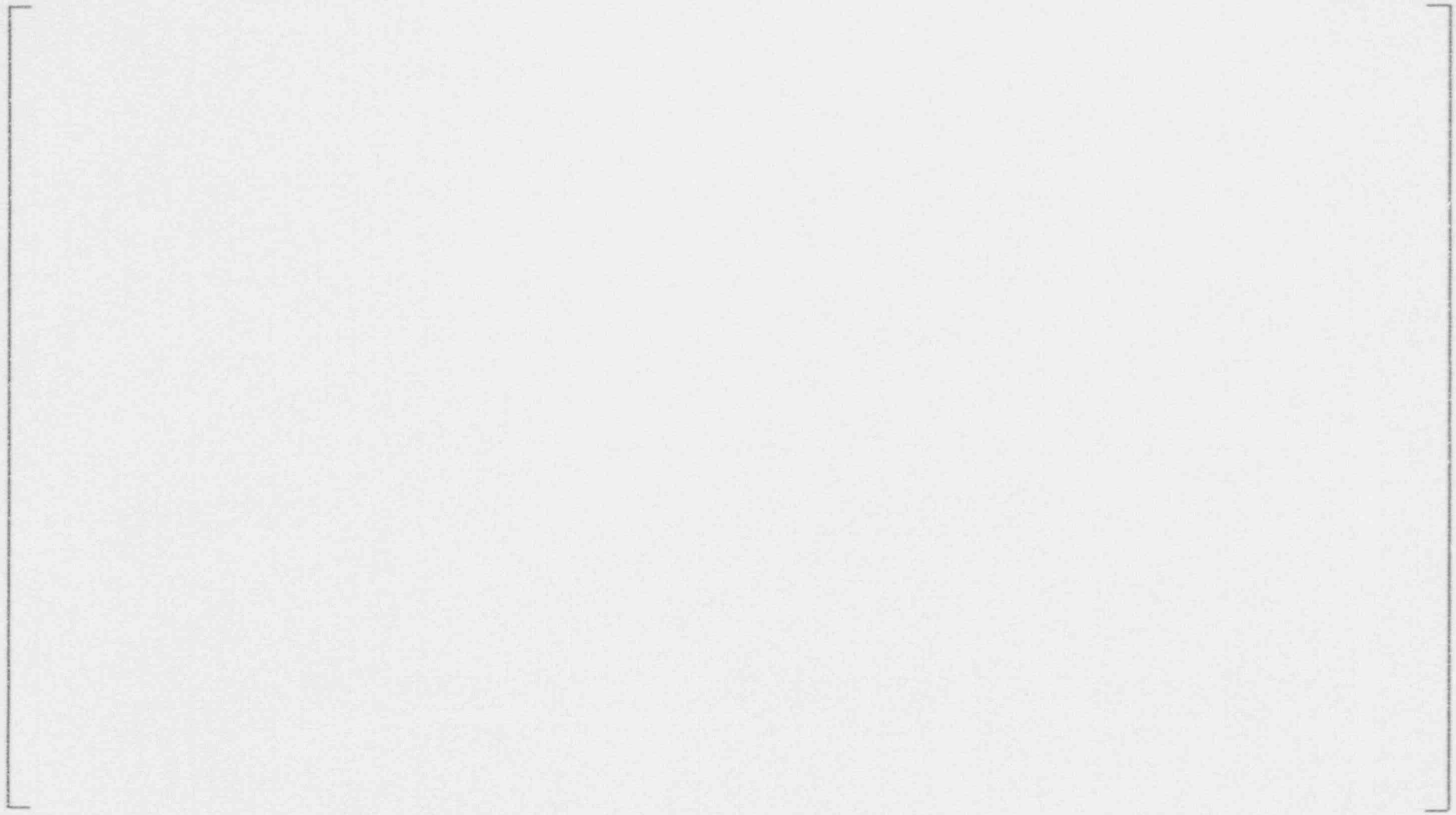

b,c

FIGURE 2-27
ALLOY 600 HEAD PENETRATION MATERIAL

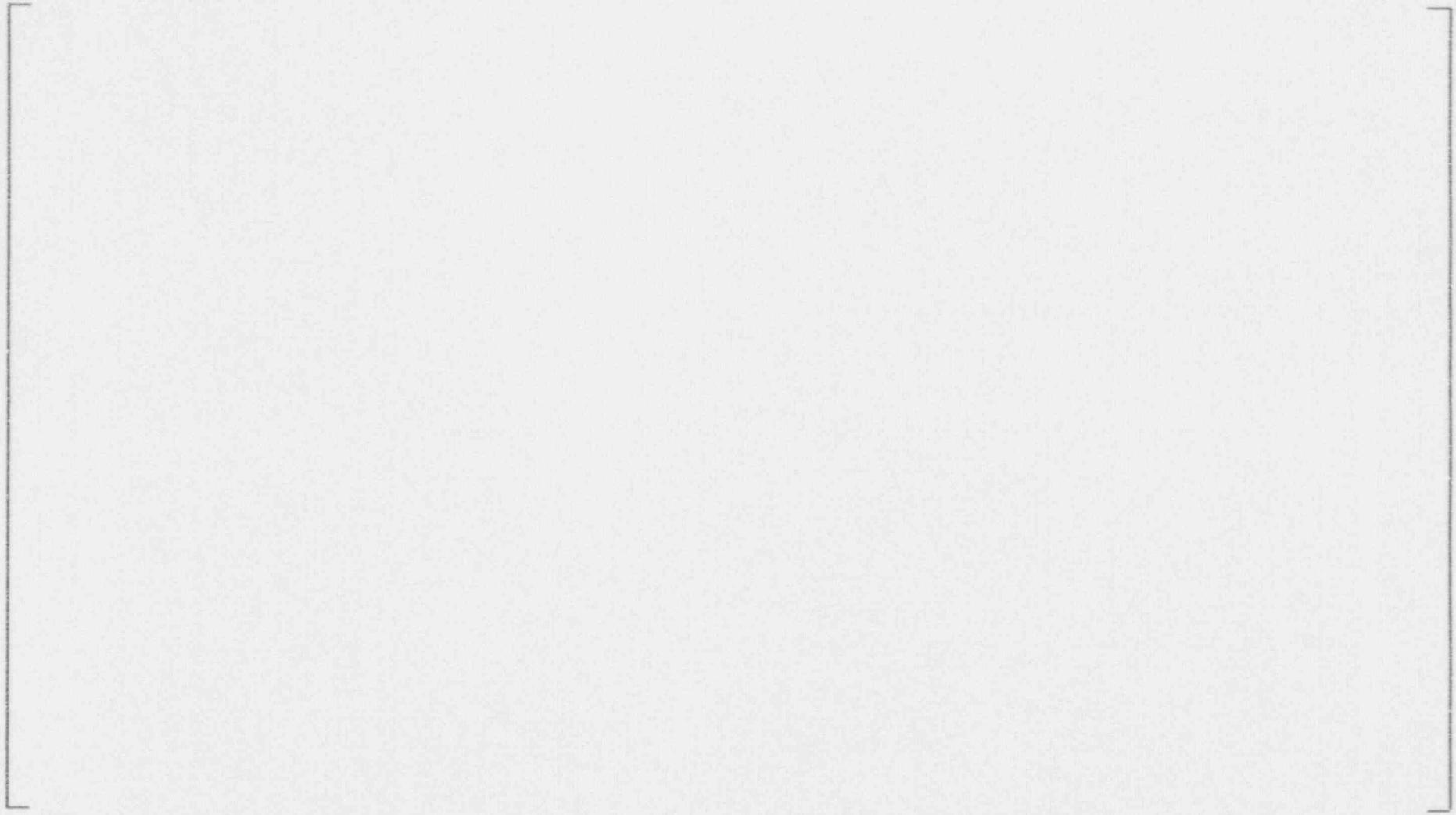

b,c

FIGURE 2-28
ALLOY 600 MATERIAL

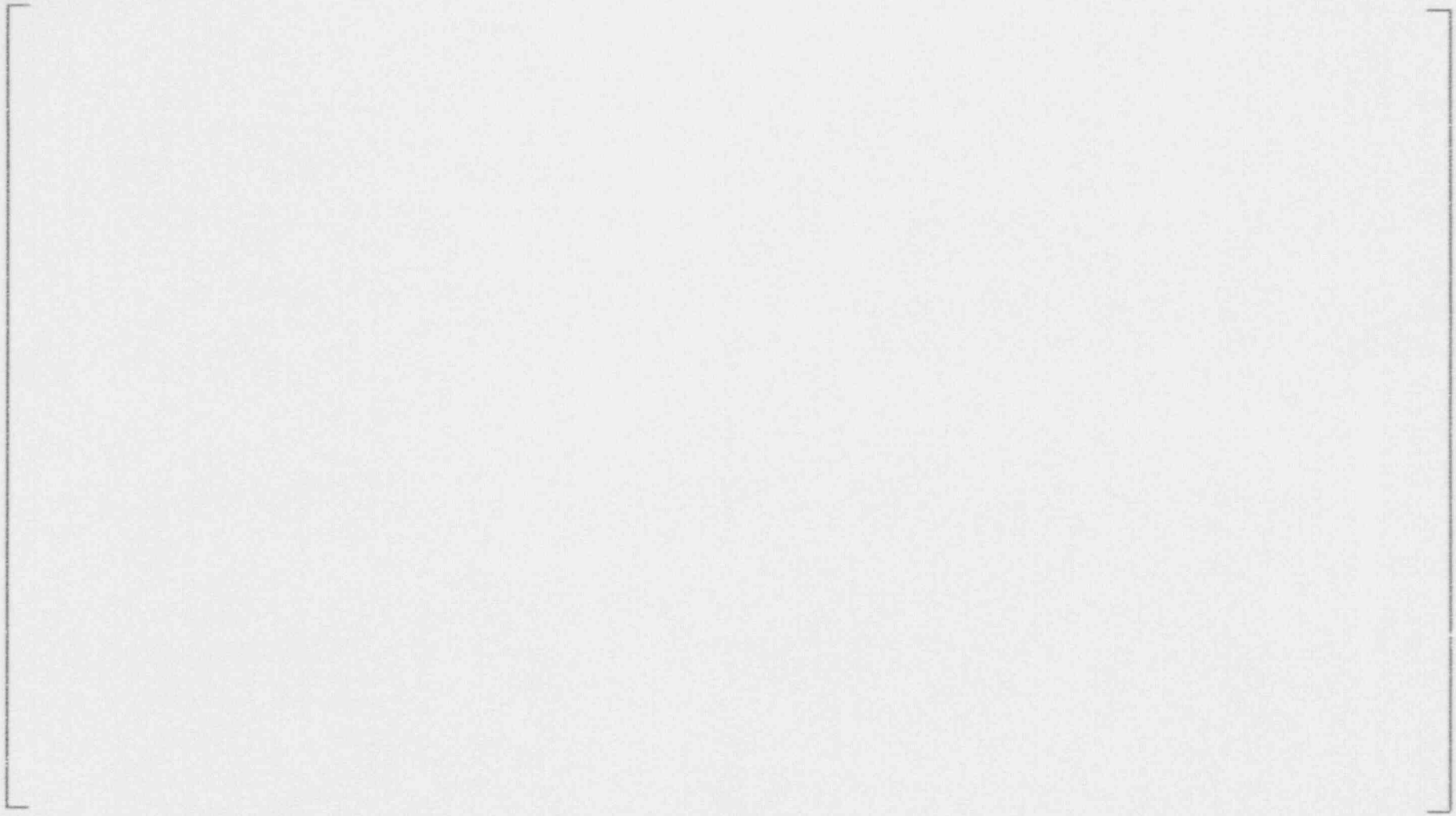

b,c

FIGURE 2-29
ALLOY 669 MATERIAL STRESS-STRAIN CURVES

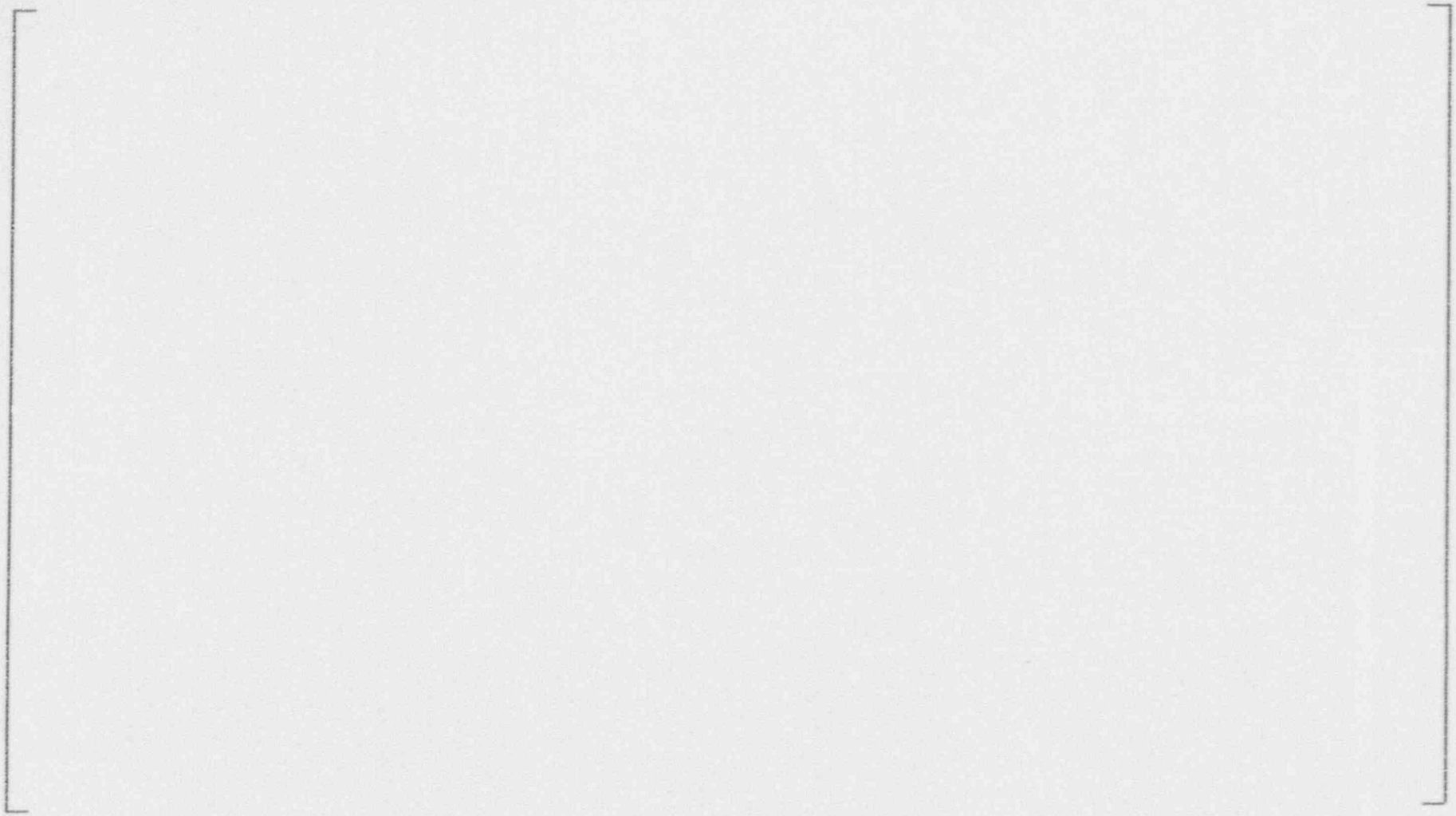

b,c

FIGURE 2-30
ESTIMATED FATIGUE CURVES FOR TEST
MATERIAL AND ACTUAL TEST DATA FOR SPECIAL TESTS

2.10 Two and Three-Loop Reactor Vessel Reconciliation

The purpose of this section is to reconcile and to demonstrate that the stresses obtained from 4-loop penetrations are enveloping for the penetrations of the 2 and 3 loop plants.

[

]b,c

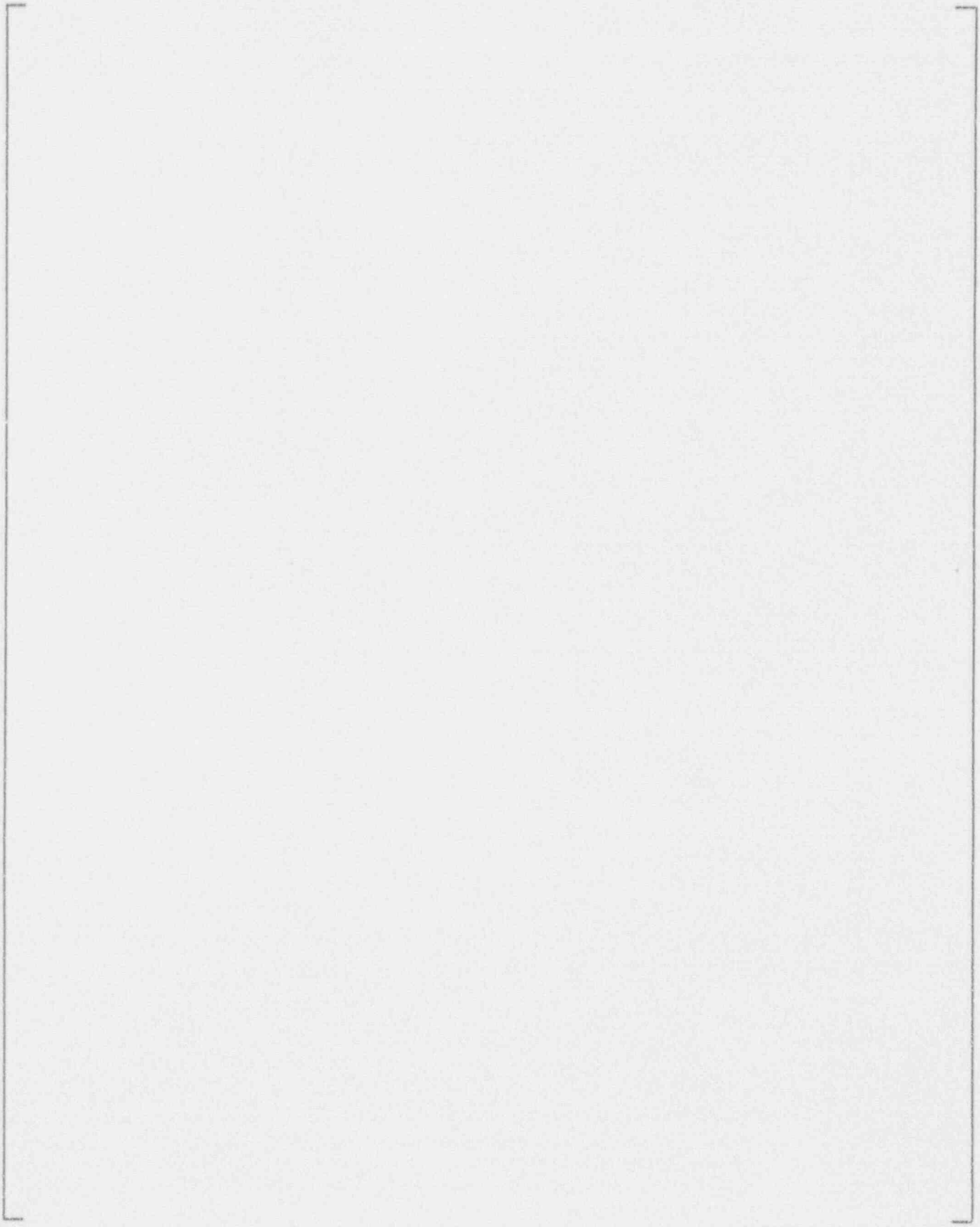

a,b,c

[

b,c

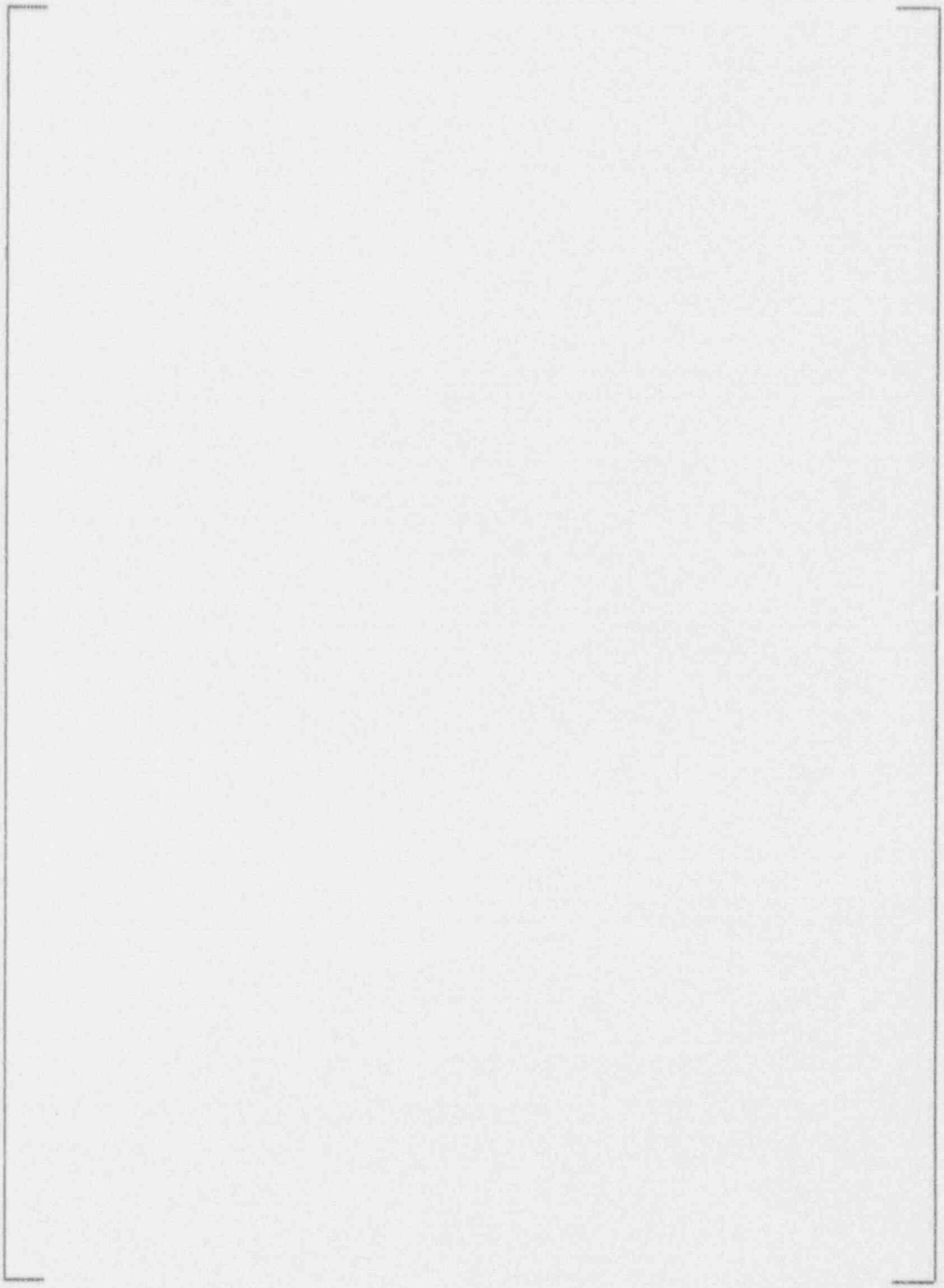

b,c

FIGURE 2-31
MAXIMUM HOOP STRESS AS A FUNCTION OF PENETRATION ANGULAR LOCATION

2.11 Summary and Conclusions

2.11.1 Summary

[

]

a,b,c

[ ]

a,b,c

2.11.2 Conclusions

[ ]

a,b,c

3.0 CRACK GROWTH ANALYSIS: FLAW TOLERANCE

3.1 Introduction

The goal of this work was to provide a quantitative measure of the tolerance of the head penetrations for the presence of a flaw. The mode of crack extension is primary water stress corrosion cracking, and therefore the loading of interest is the steady state operating condition. The crack growth law used in this study was obtained from a survey of the available literature on this material and environment, with the temperature effect on the growth rates based on a collection of crack growth information from both laboratory and field data.

3.2 Crack Growth Prediction Methodology

[a,b,c]

Scott's model appears to follow the appropriate trends, and was therefore chosen as the best available model for prediction of the crack growth in the penetrations. The equation for the model at 330°C (6.26°F) is:

[ ]

a,b,c

3.3 Overall Approach

[ ]

a,b,c

[ ] a,c

3.4 Results

[ ] a,b,c

3.5 Summary and Conclusions

[ ] a,c

[

]

a,b,c

Table 3-1

Temperature Correction Factors for Crack Growth: Alloy 600

[ ] b,c

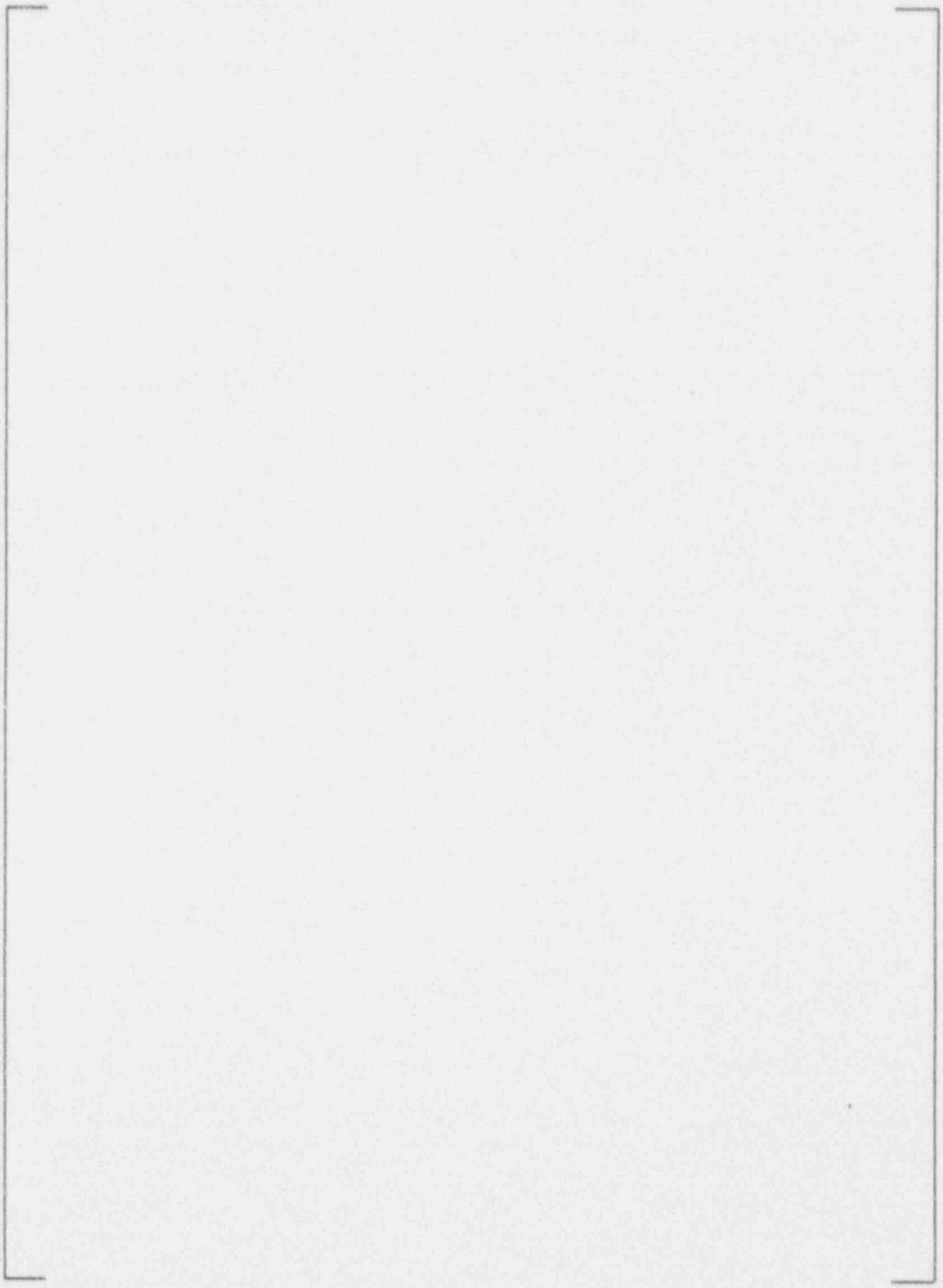

b,c

FIGURE 3-1
CRACK GROWTH RATE MEASUREMENTS IN THE
1200 ppm B, 2.2 ppm Li BASELINE ENVIRONMENT[1]

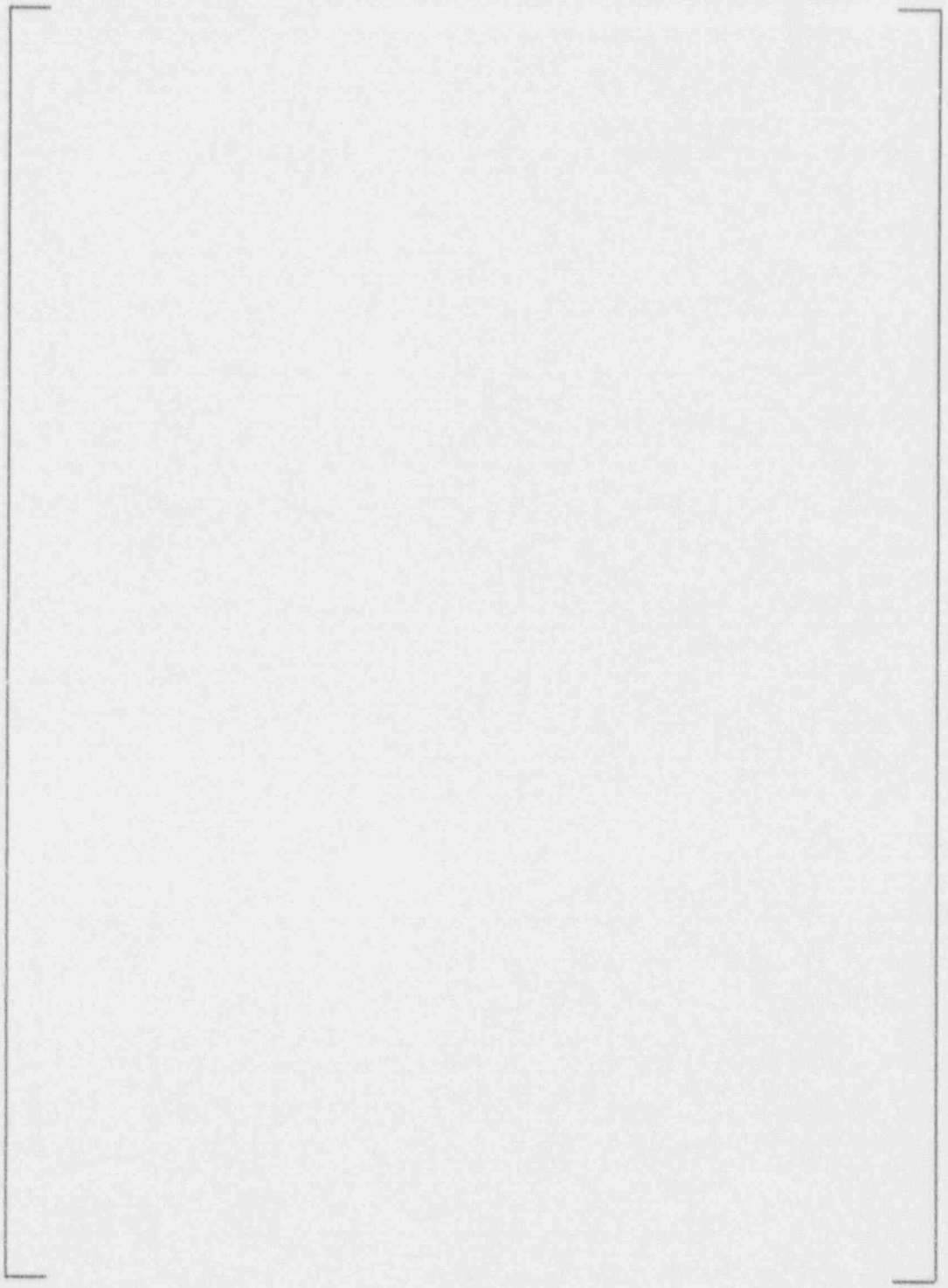

b,c

FIGURE 3-2
CRACK GROWTH RATE RESULTS FOR STATICALLY AND ACTIVELY LOADED SPECIMENS IN THREE DIFFERENT ENVIRONMENTS[1]

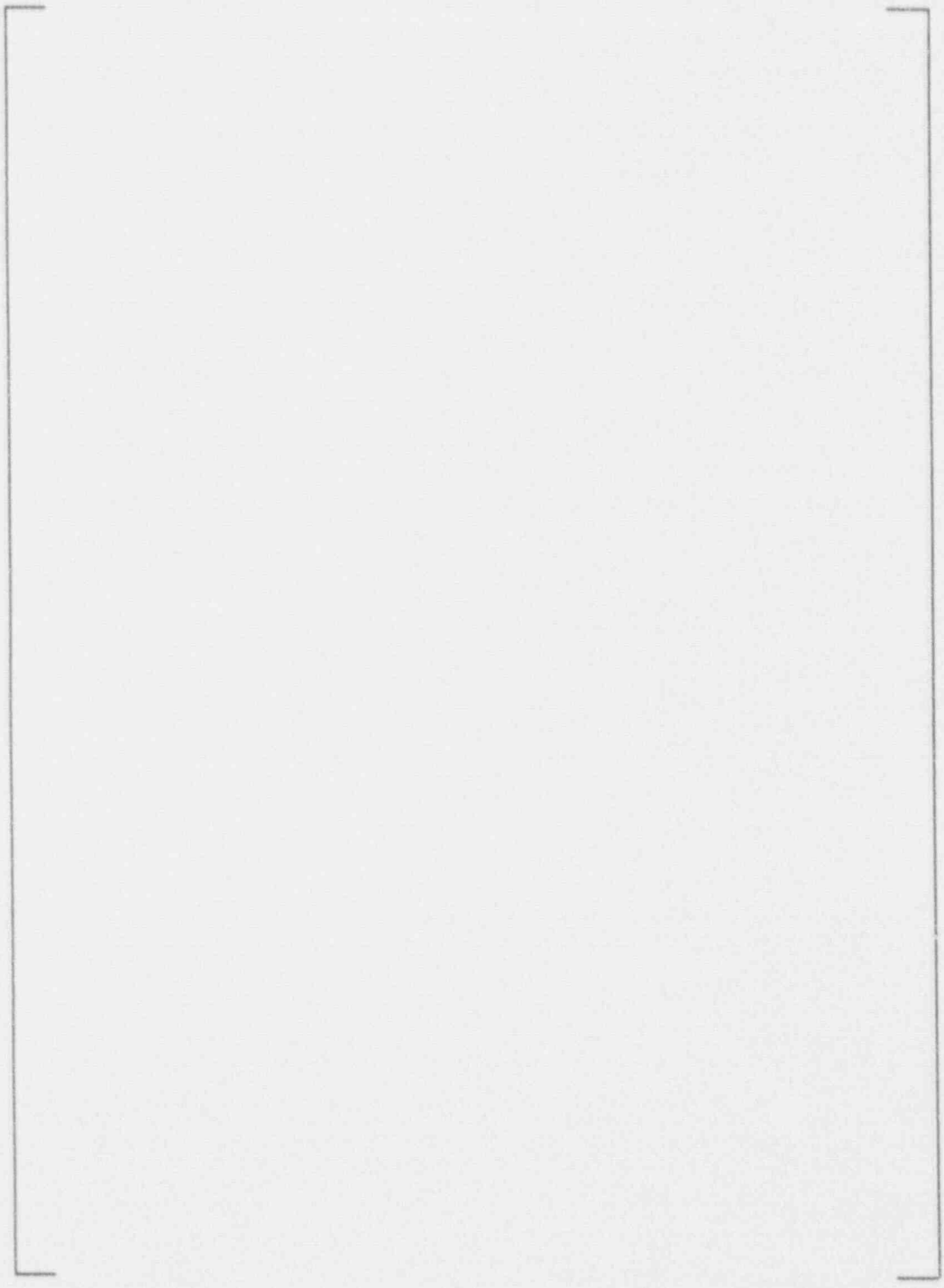

b,c

FIGURE 3-3
SCOTTS MODEL[2] FOR SCC GROWTH RATES IN ALLOY 600 IN
PRIMARY WATER ENVIRONMENTS (330°C)

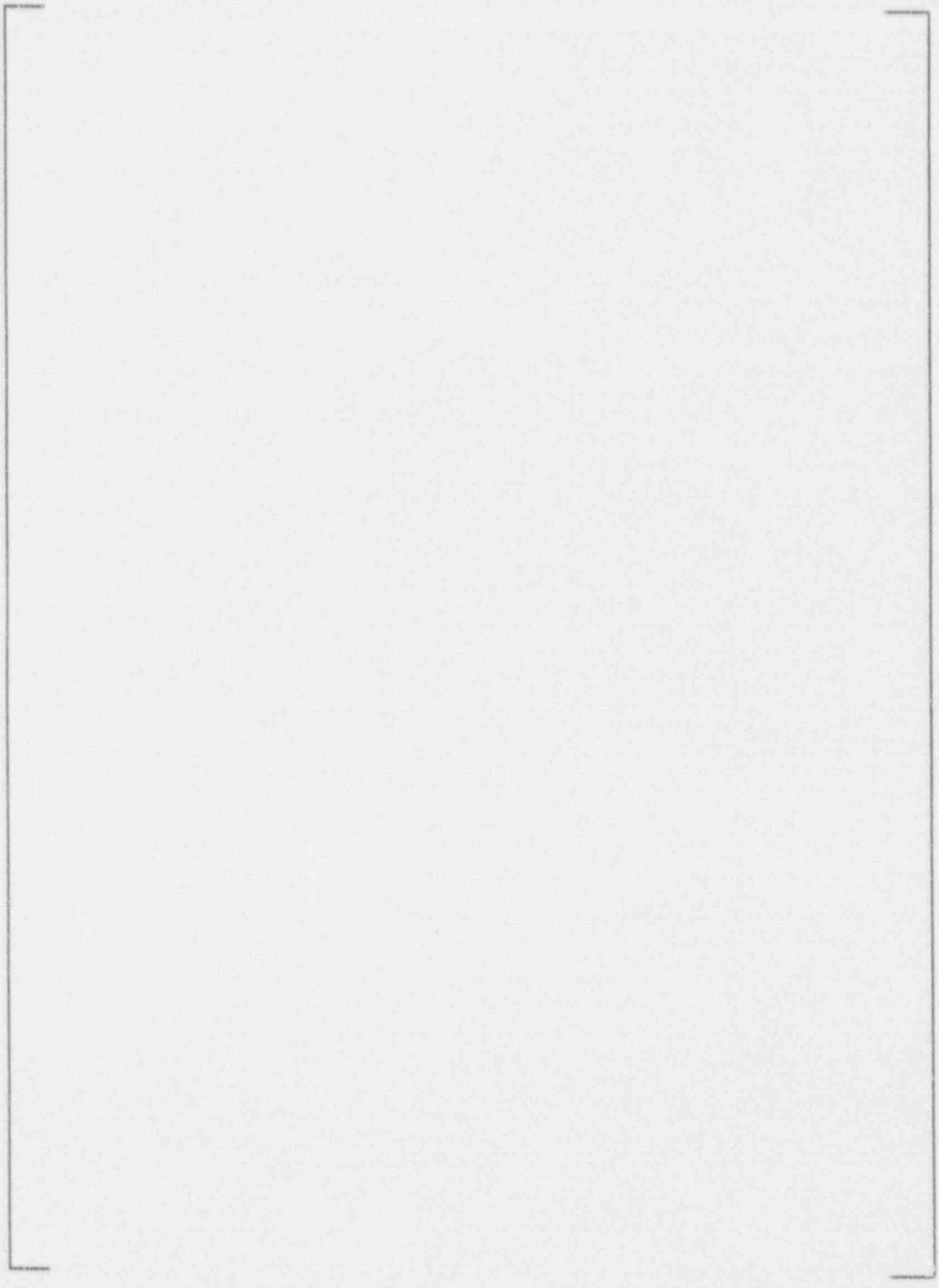

b,c

FIGURE 3-4
VALIDATION OF CRACK GROWTH LAW WITH FIELD DATA

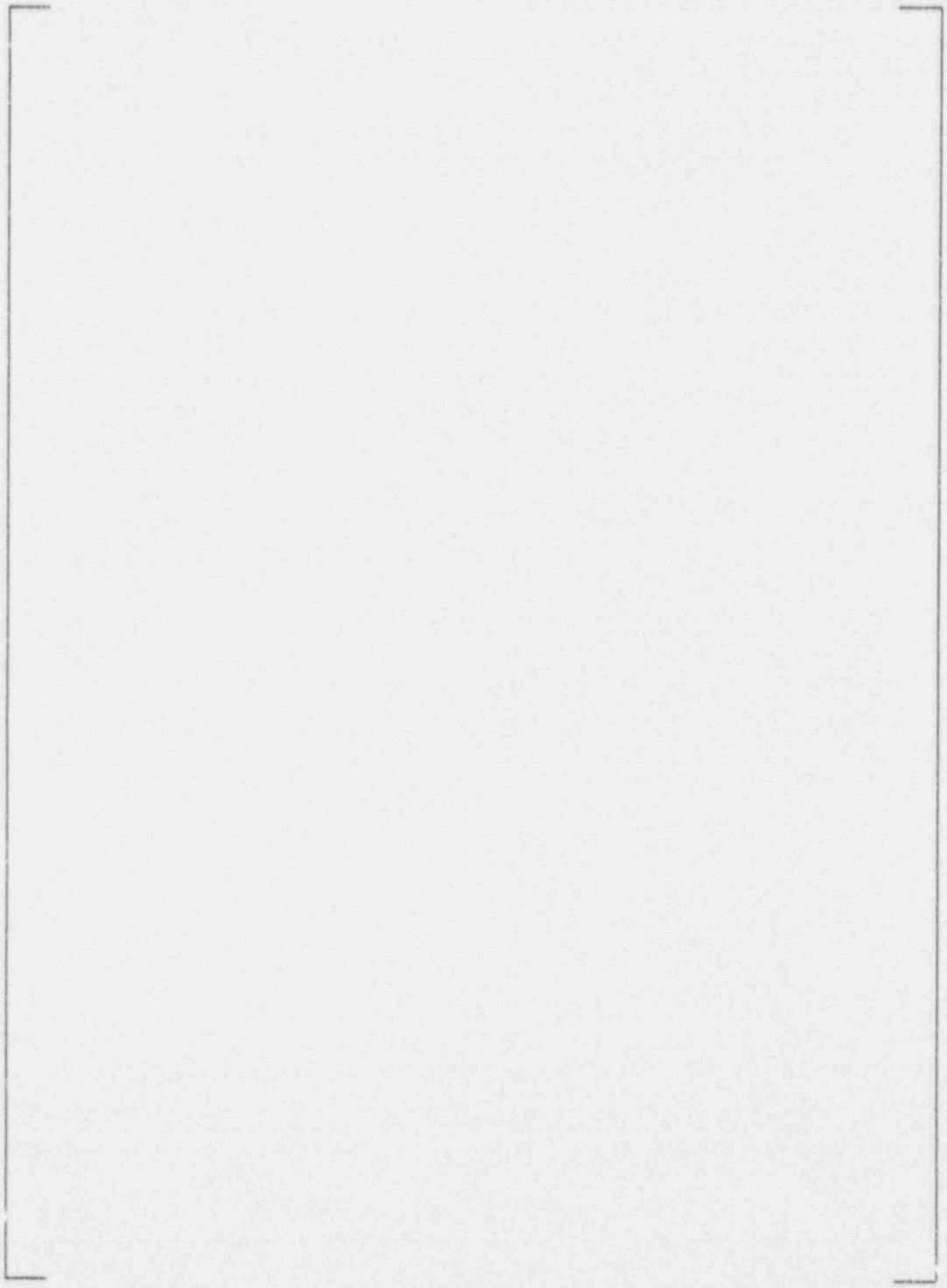

b,c

FIGURE 3-5
SUMMARY OF TEMPERATURE EFFECTS ON SCC GROWTH RATES FOR
ALLOY 600 IN PRIMARY WATER, LABORATORY AND FIELD EXPERIENCE

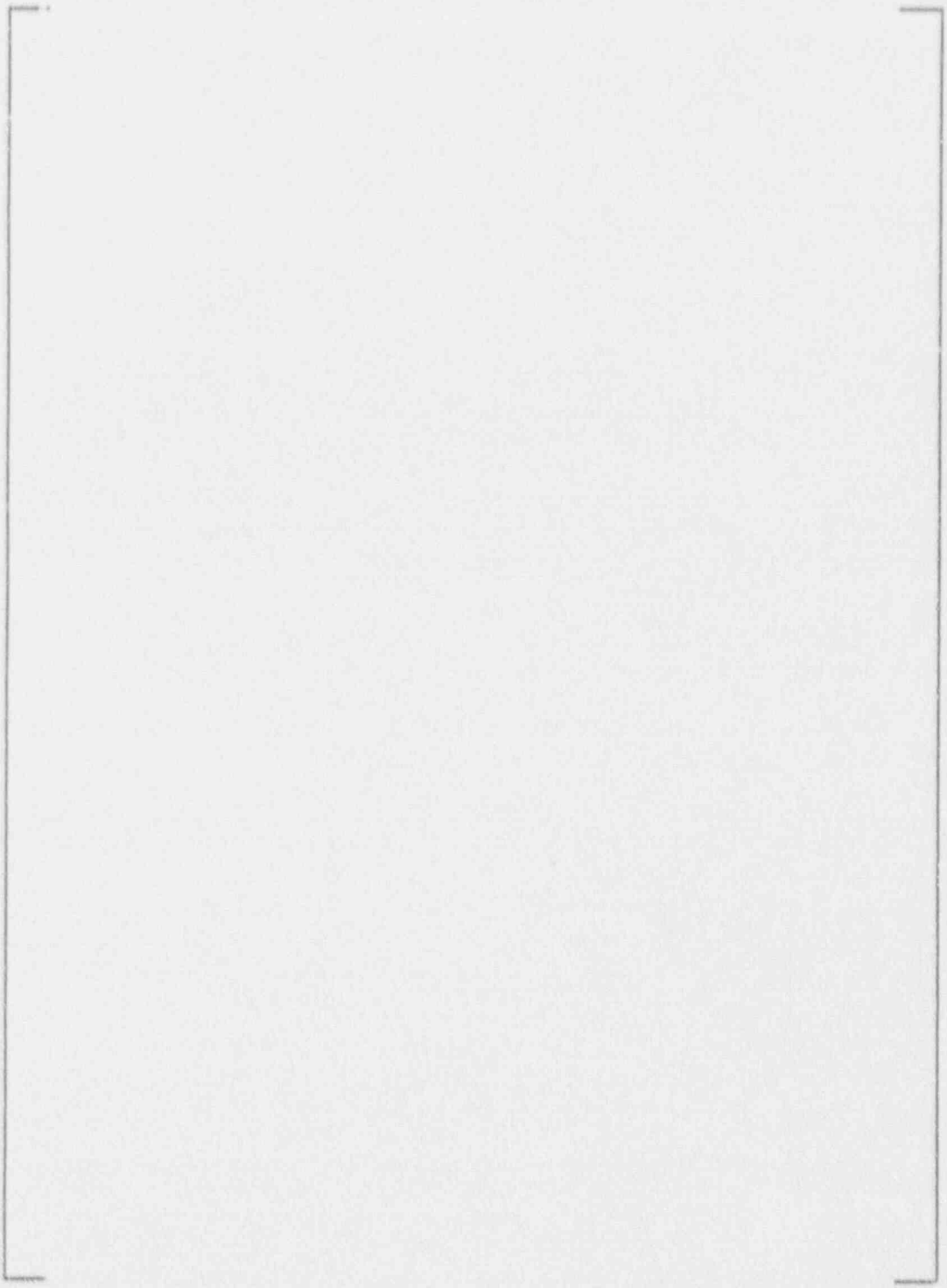

b,c

FIGURE 3-6
CRACK GROWTH PREDICTIONS FOR SURFACE FLAWS BELOW AND AT THE WELD REGION IN THE HEAD PENETRATIONS FOR A RANGE OF TEMPERATURES

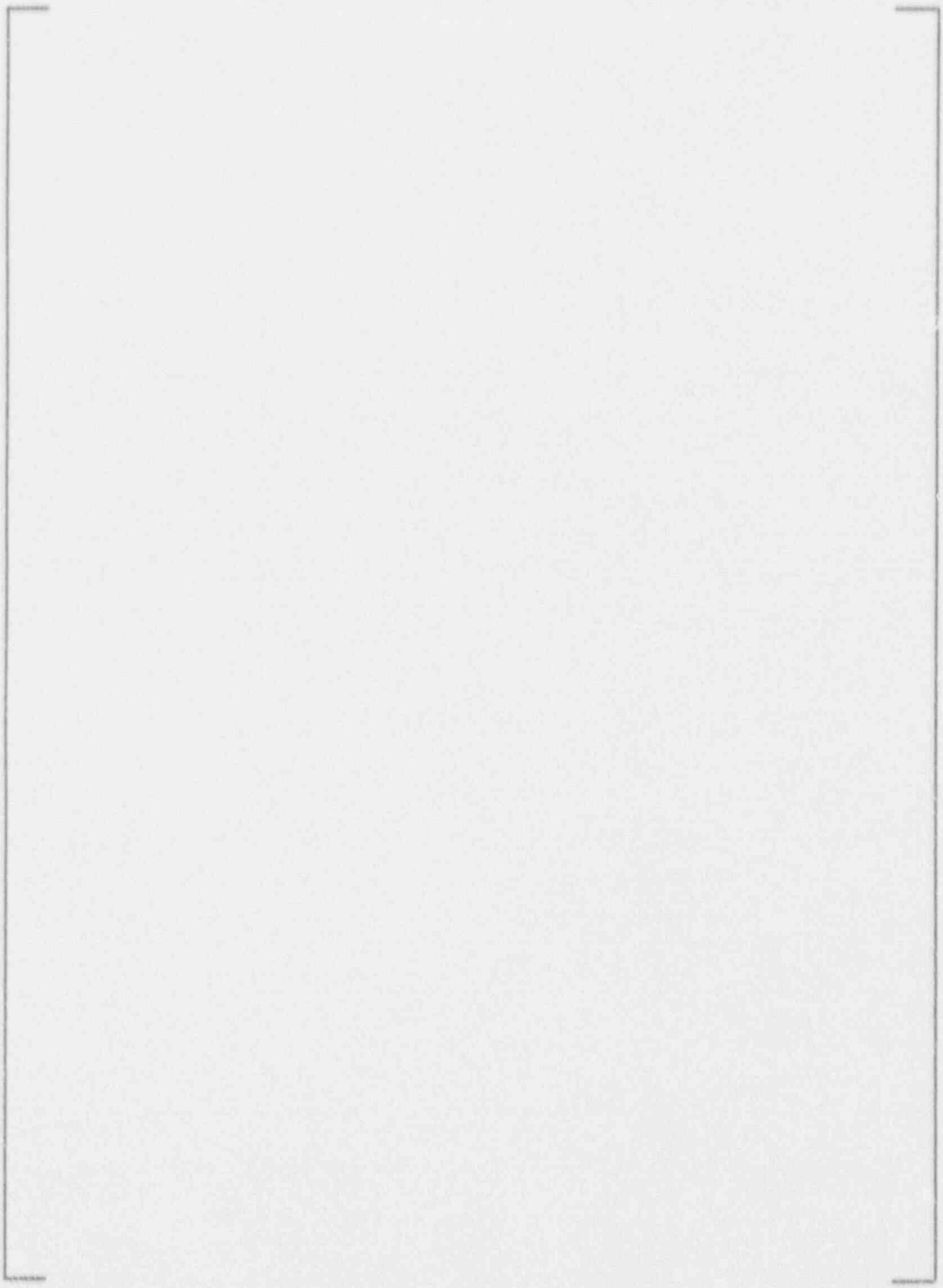

b,c

FIGURE 3-7
CRACK GROWTH PREDICTIONS FOR THROUGH-WALL FLAWS
LOCATED AT THE CENTER SIDE OF THE OUTERMOST HEAD PENETRATIONS
FOR A RANGE OF TEMPERATURES

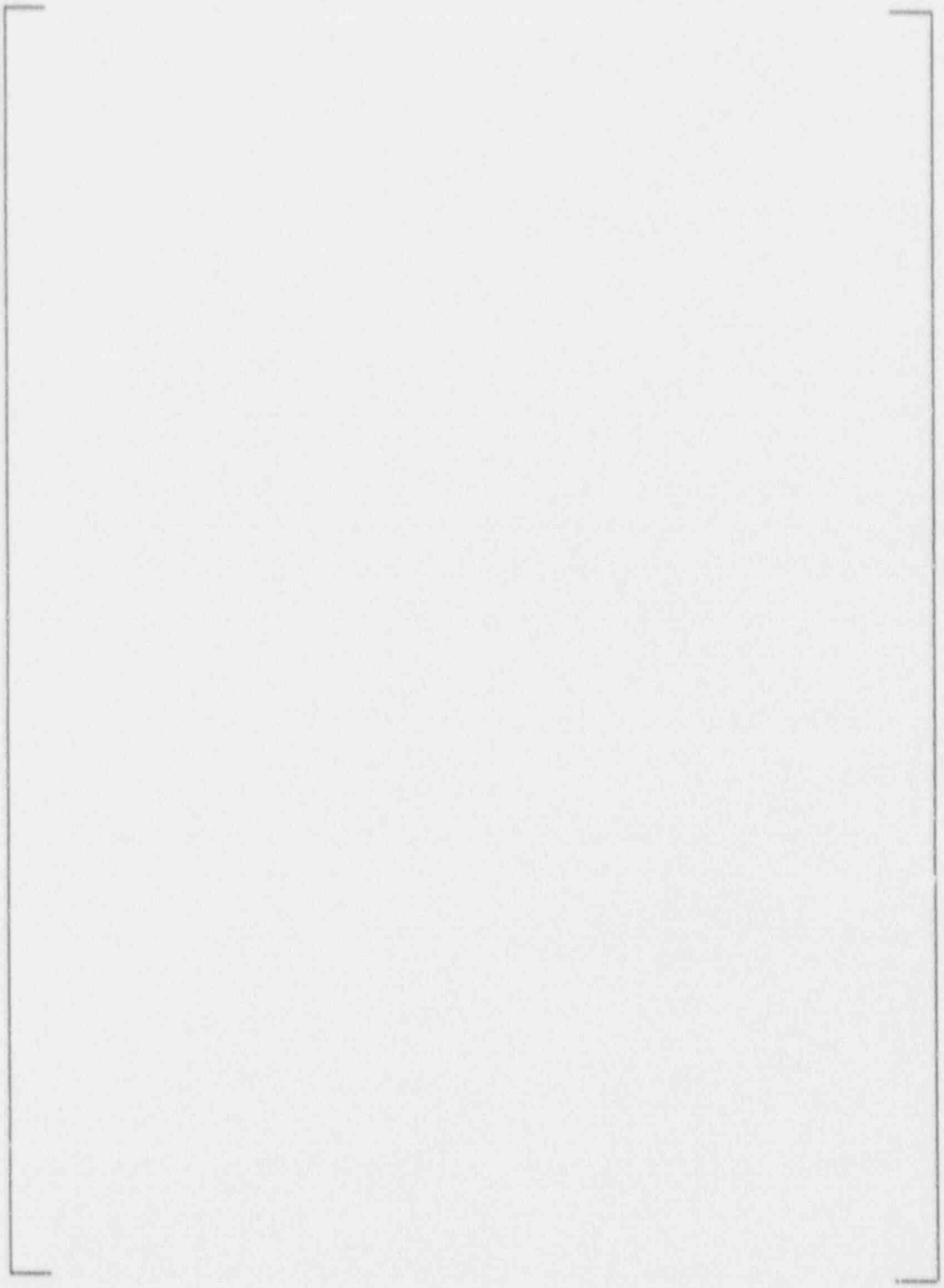

b,c

FIGURE 3-8
CRACK GROWTH PREDICTIONS FOR THROUGH-WALL FLAWS LOCATED ON THE LOWER HILLSIDE OF THE OUTERMOST HEAD PENETRATIONS, FOR A RANGE OF TEMPERATURES

4.0 PENETRATION LEAKAGE ASSESSMENT

a,b,c

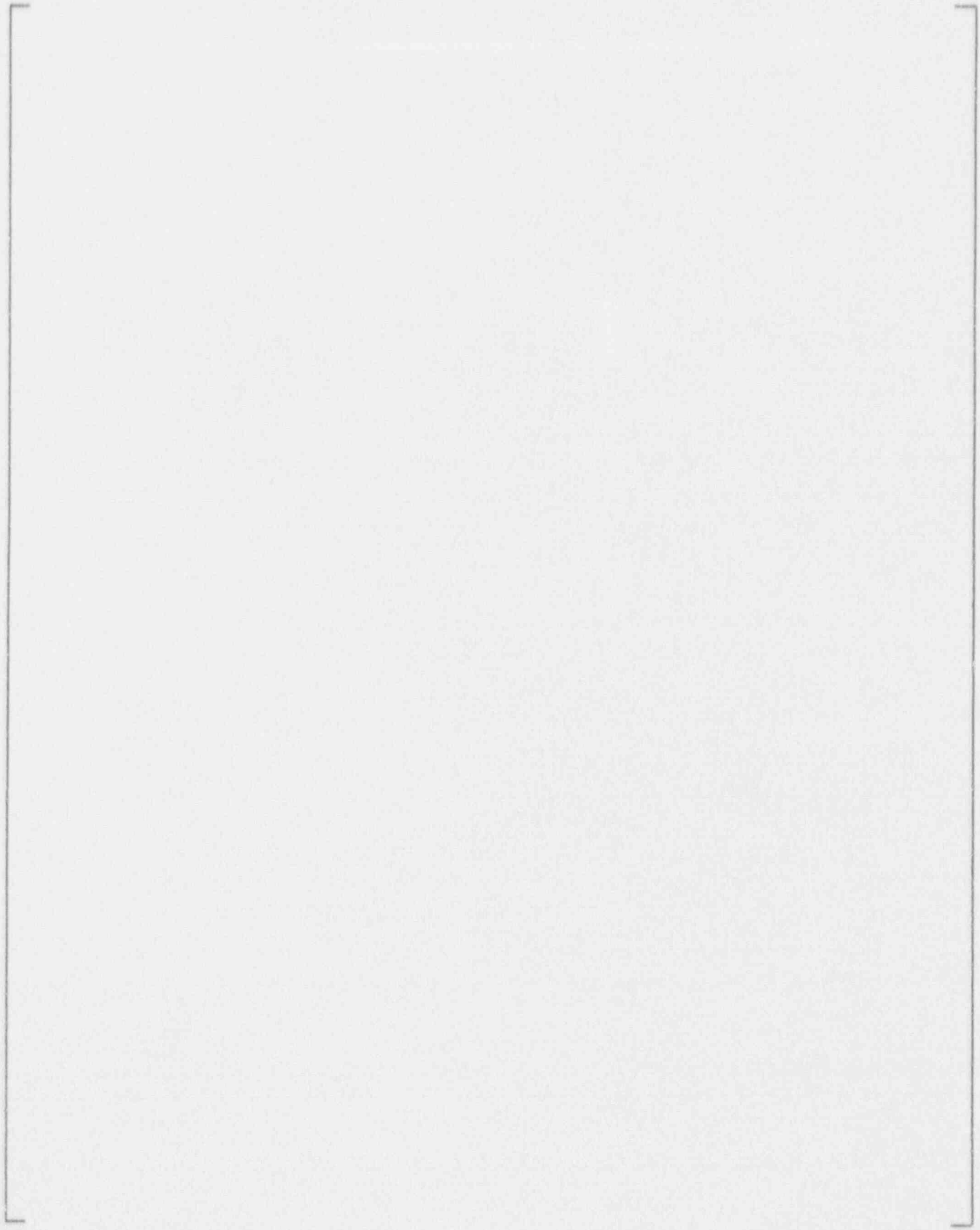

a,b,c

[

]

a,b,c

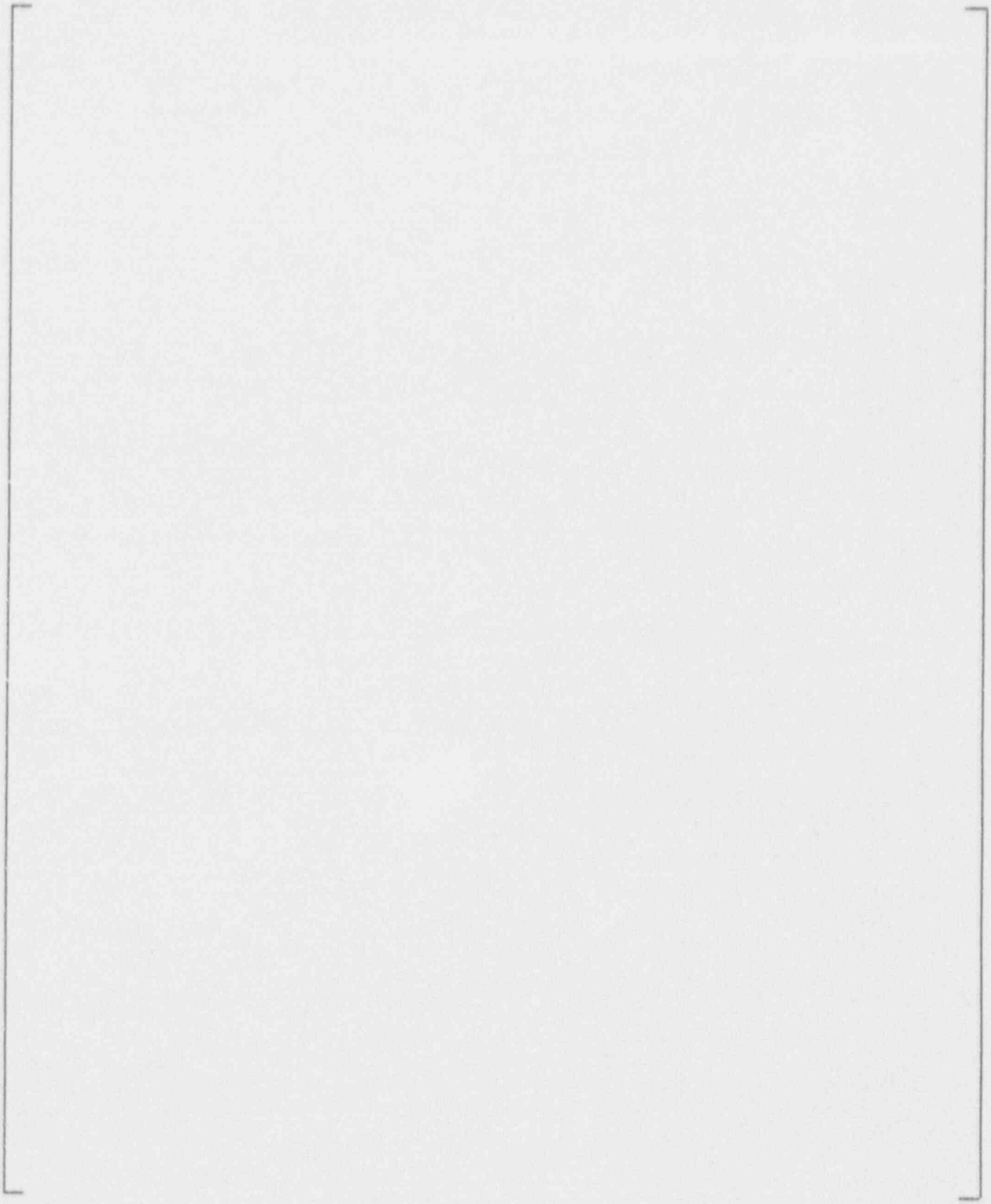

a,b,c

[

]

a,b,c

[

]

b,c

a,b,c

Table 4-1

Leak Rates Through a Range of Crack Lengths: Head Penetration

[ ] b,c

Table 4-2
Crack Length, Mass Flux and Heat Capacity Ratio
in the Annulus Clearance Between Penetration and Vessel

[ ]

b,c

Table 4-3
Leak Rate Through the Annular Clearance Between the Head Penetration and Vessel

b,c

Table 4-4
Leak Rate Through the Annular Clearance Between the Head Penetration and Vessel

[ ]

b,c

Table 4-4 (cont)
Leak Rate Through the Annular Clearance Between the Head Penetration and Vessel

[ ]

b,c

Table 4-5
Final Leak Rate Calculation for Penetration with Reported Leak
(Longitudinal Flaw at Temperature = 150°F - Single Phase Flow)

b,c

Table 4-5 (cont)
Final Leak Rate Calculation for Penetration with Reported Leak
(Longitudinal Flaw at Temperature = 150°F - Single Phase Flow)

[ ]

b,c

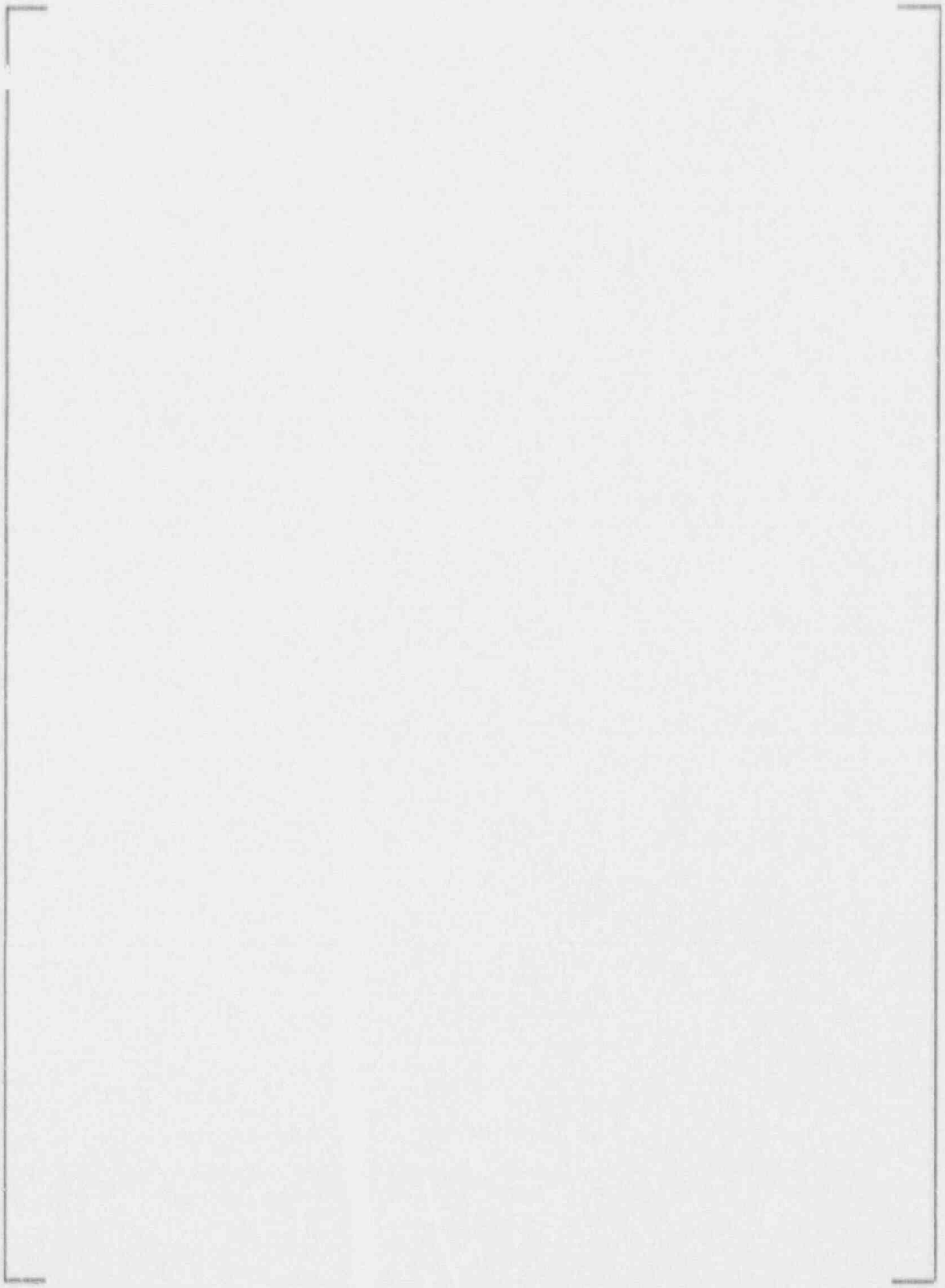

a,c

FIGURE 4-1
HEAD PENETRATION AND VESSEL ASSEMBLY

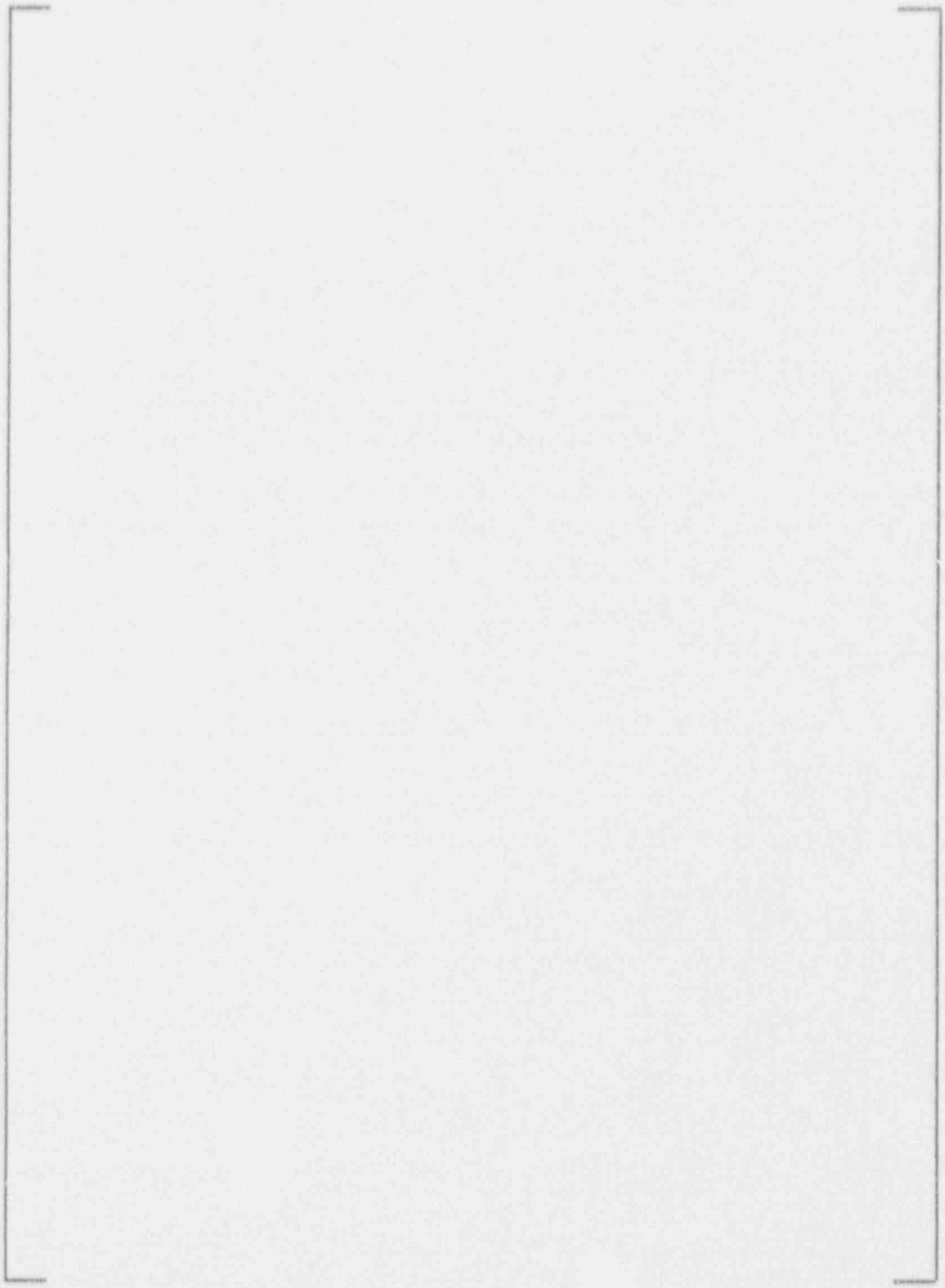

b,c

FIGURE 4.2
LEAK RATE AS A FUNCTION OF CLEARANCE AND CRACK
LENGTHS IN TERMS OF LITERS PER MINUTE AT THE EXIT OF
ANNULUS CLEARANCE BETWEEN HEAD PENETRATION AND VESSEL

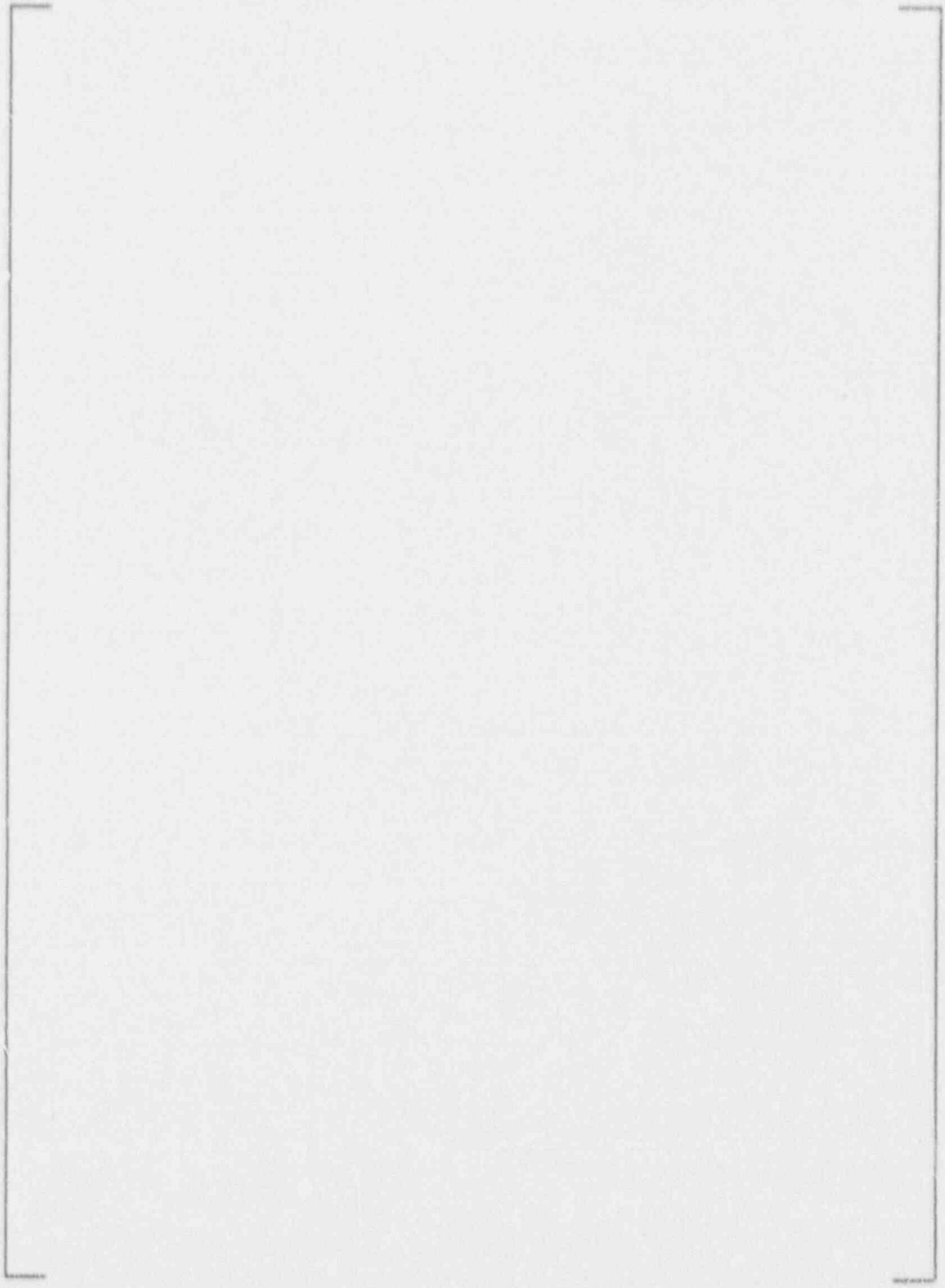

b,c

FIGURE 4-3
LEAK RATE AS A FUNCTION OF CLEARANCE
AND CRACK LENGTHS IN TERMS OF GPM AT THE EXIT
ANNULUS CLEARANCE BETWEEN HEAD PENETRATION AND VESSEL

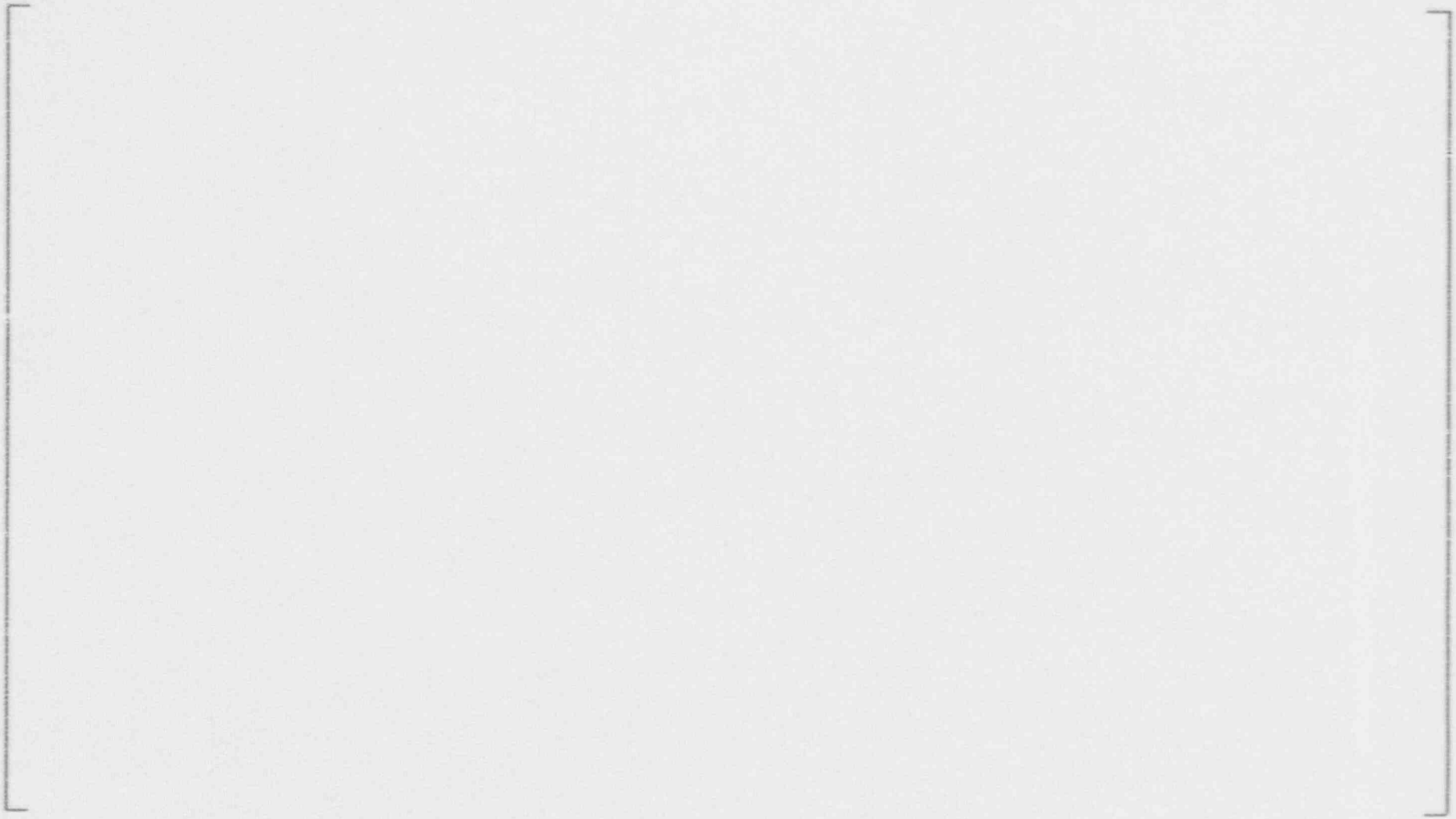

b,c

FIGURE 4-4
PREDICTED LEAK RATE FOR HYDROTEST CONDITIONS - SHORT CRACKS

b,c

FIGURE 4-5
PREDICTED LEAK RATE FOR HYDROTEST CONDITIONS - LARGE CRACKS

4.2 Reactor Vessel Head Wastage Assessments/Comparison to ASME Code Allowables

[

]b,c

b,c

[

]b,c

[

]b,c

[ ]b,c

Table 4-6
Summary of Wastage Evaluation Stress Analysis

[ ]

b,c

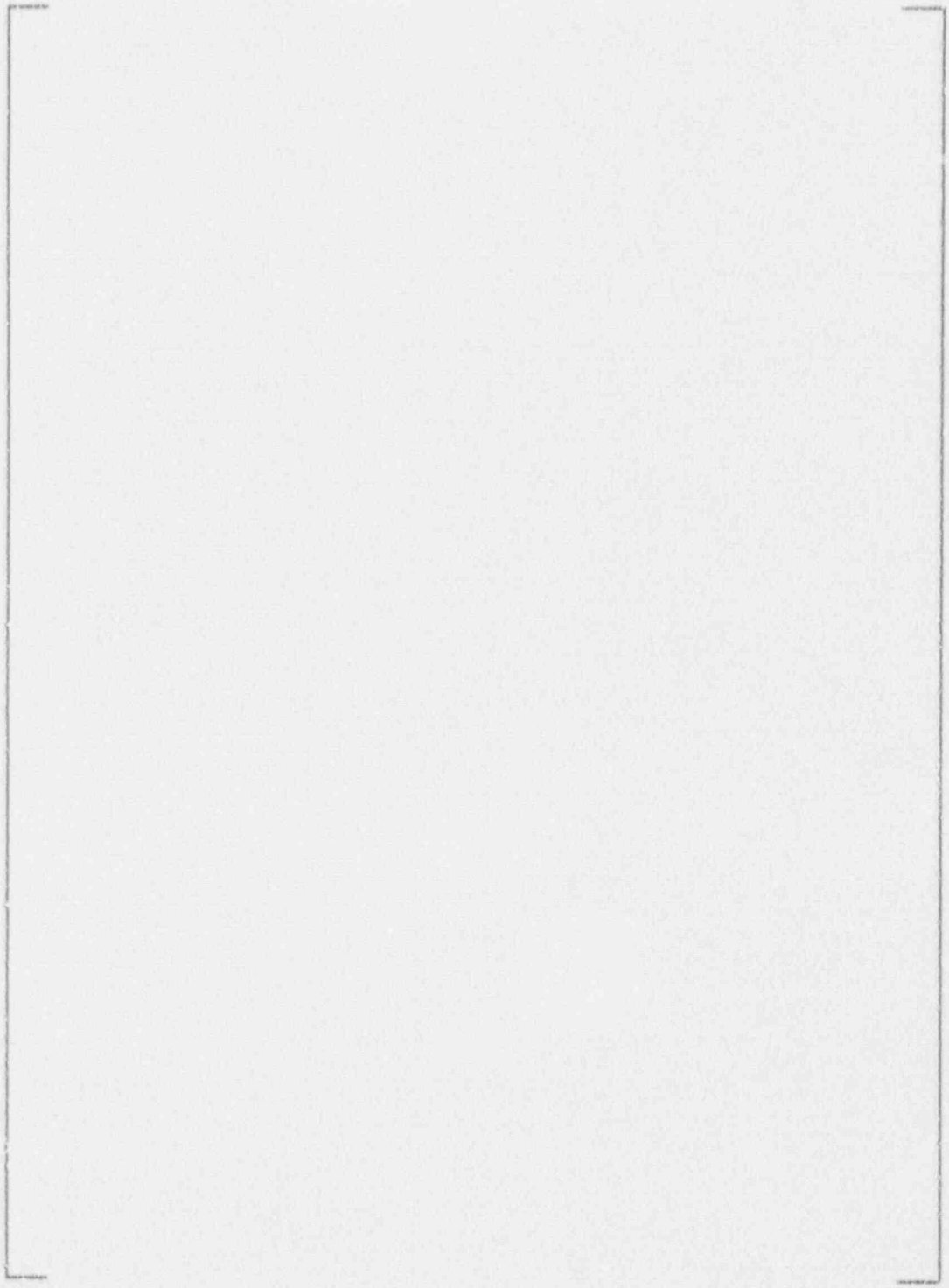

b,c

FIGURE 4-6
WOG PLANT REACTOR VESSEL HEAD PENETRATION LEAKAGE -
POSTULATED WASTAGE DEFECT GEOMETRIES

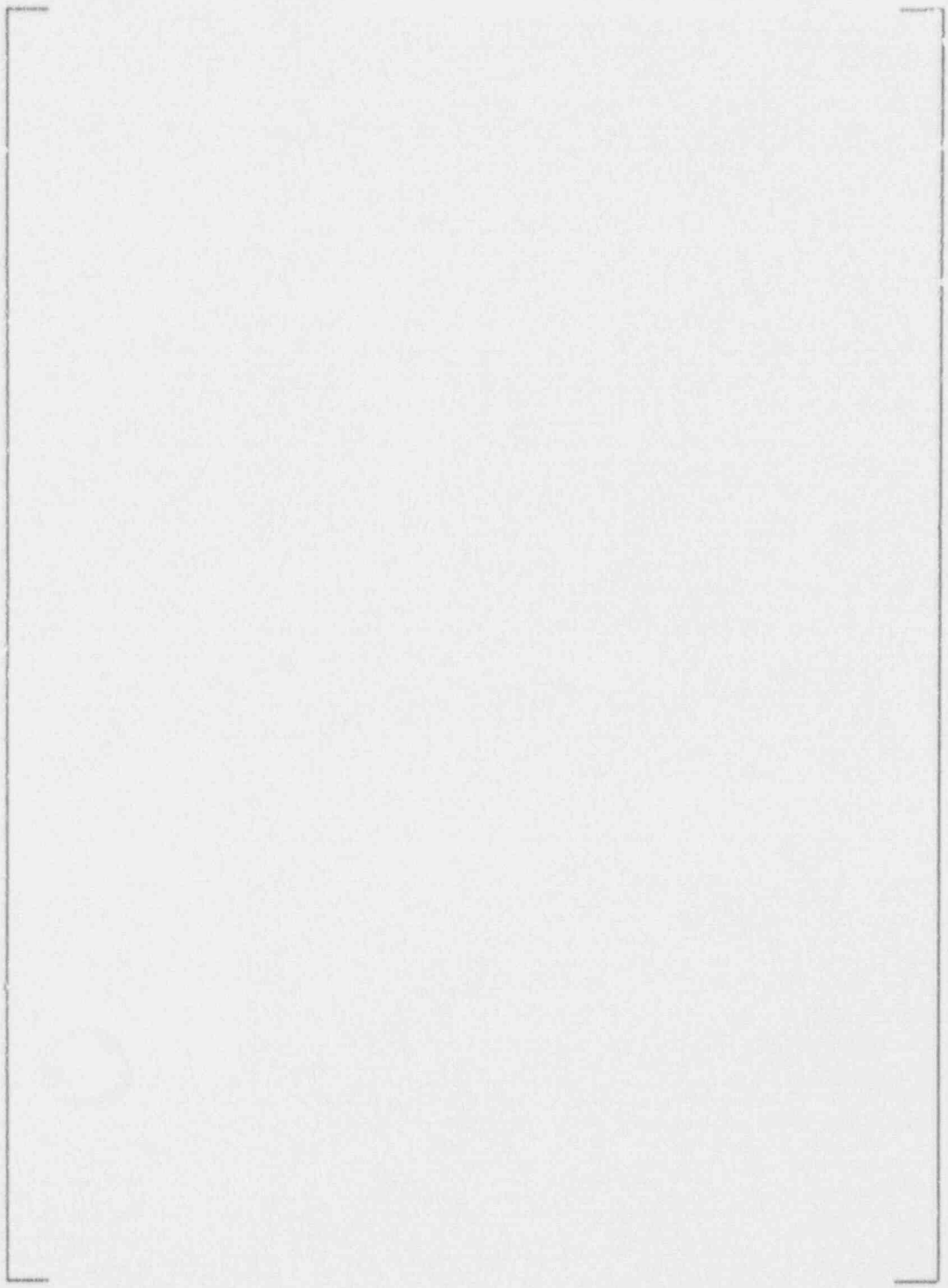

a,c

FIGURE 4-7
REACTOR VESSEL HEAD WASTAGE ANALYSIS MODEL FOR FOUR LOOP HEAD

5.0 PLANT/PENETRATION CATEGORIZATION/PENETRATION INSPECTIONS

[

]

b,c,g

5.1.2 Applicability to WOG Plants

[ ]

b,c,g

5.1.3 Estimate of Condition of WOG Plant Penetrations

[ ]

b,c,g

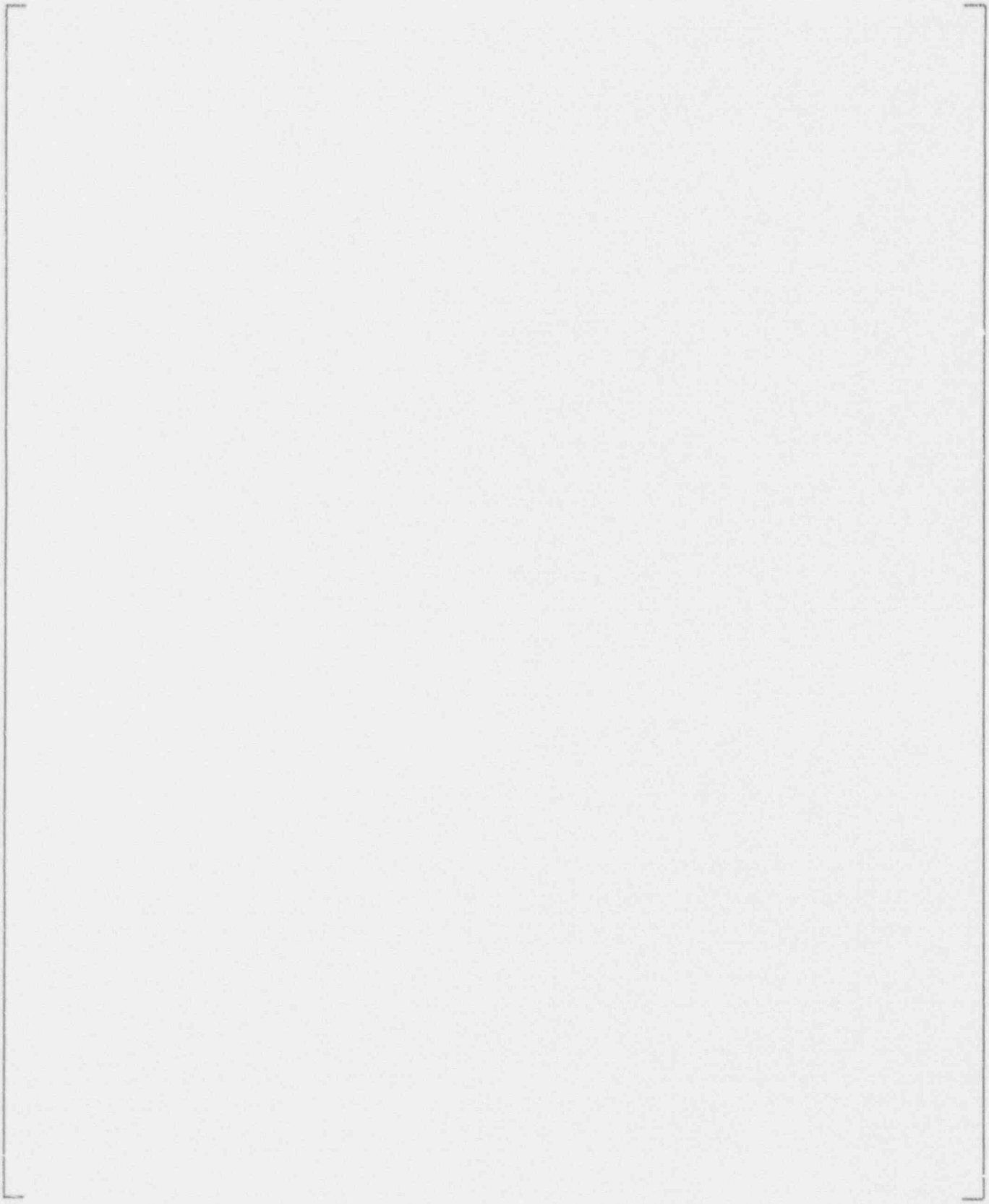

b,c,g

[

]

b,c,g

5.1.4 Results and Conclusions

[

]

b,c,g

[

]

5.2 Microstructure Characterization Studies

b,c,g

[

]

a,c,g

5.2.1 Metallography and Hardness Traverse Measurements

[

]

b,c

[

]

a,c,g

5.2.2 Results and Discussion

[

]

a,b,c,g

Table 5-1
Summary of Metallography Results on Alloy 600
Penetration Tube Materials

[

]

b,c,g

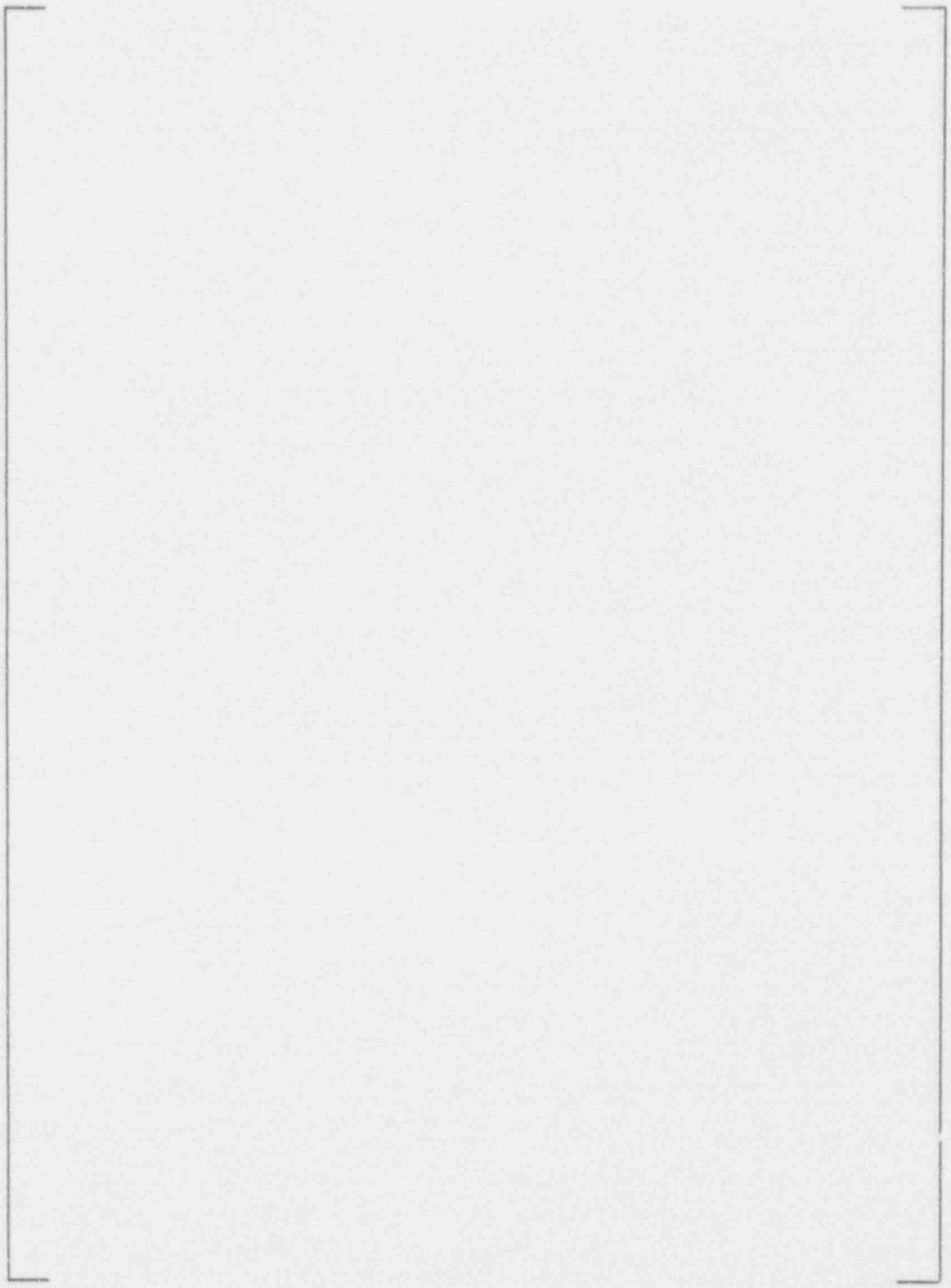

b,c

FIGURE 5-1
KNOOP HARDNESS TRAVERSES ON THE TRANSVERSE CROSS-SECTION OF
A JAMESPORT PENETRATION TUBE WALL STARTING AT A GROUND SURFACE
AND AT A MACHINED SURFACE

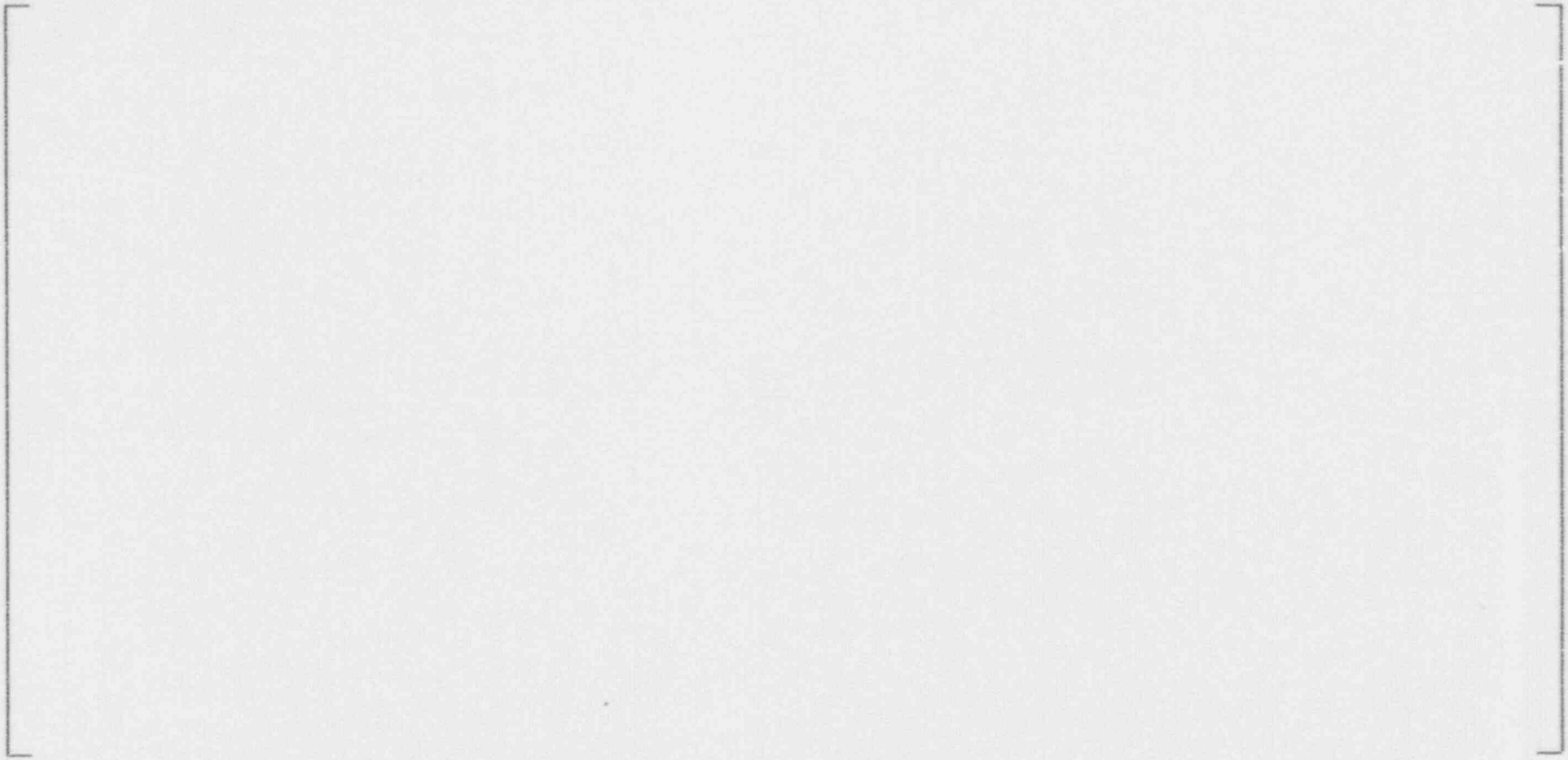

b,c

FIGURE 5-2

SEM MICROGRAPHS ILLUSTRATING
THE MICROSTRUCTURE OF THE
ALLOY 600 SAMPLE OBTAINED FROM
THE BEAVER VALLEY STATION PENETRATION
TUBE CALIBRATION STANDARD (BROMINE ETCH)

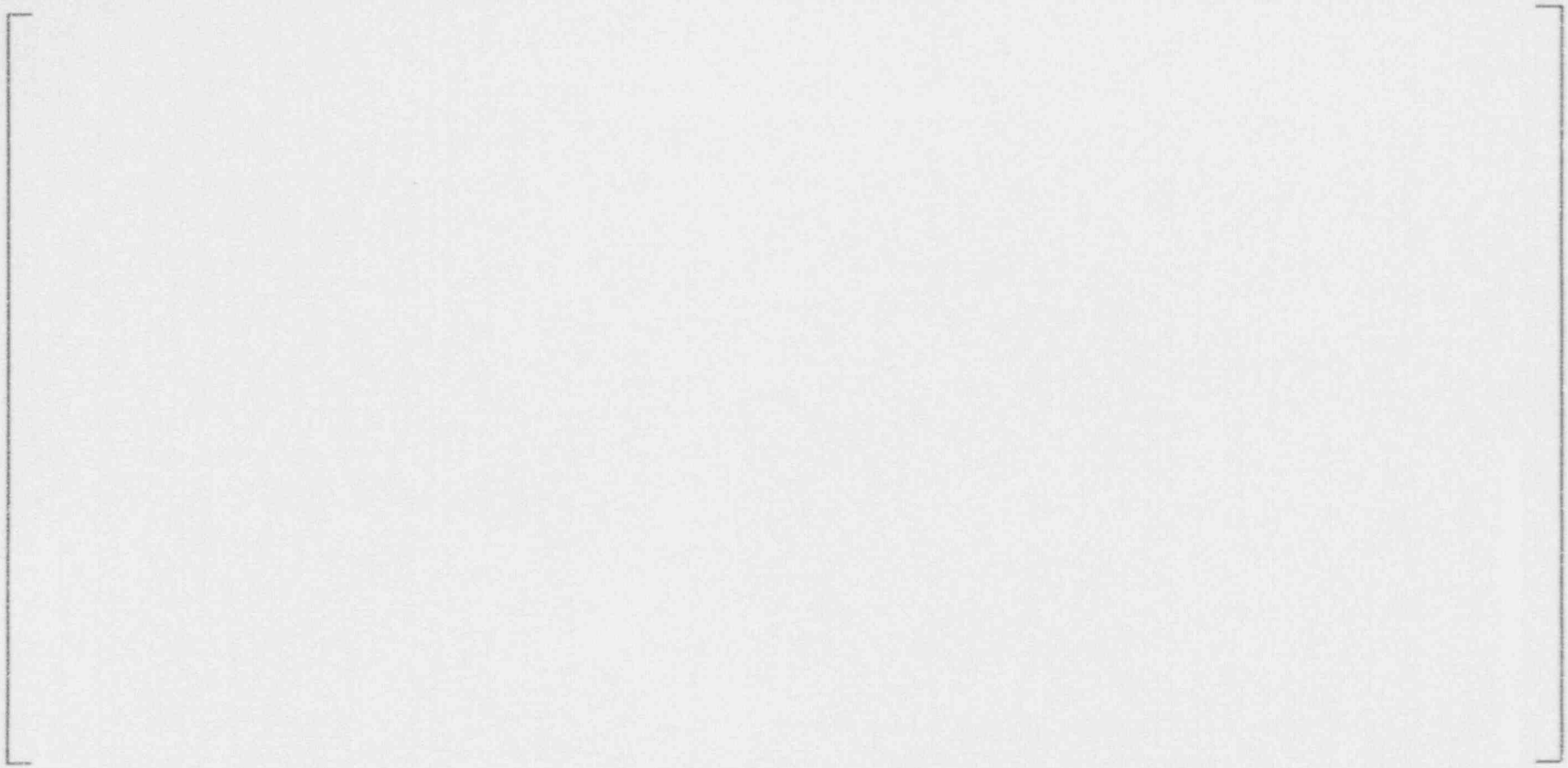

b,c

FIGURE 5-3

SEM MICROGRAPHS ILLUSTRATING
THE MICROSTRUCTURE OF THE
ALLOY 600 SAMPLE OBTAINED FROM
THE VOGTLE STATION PENETRATION
TUBE CALIBRATION STANDARD (BROMINE ETCH)

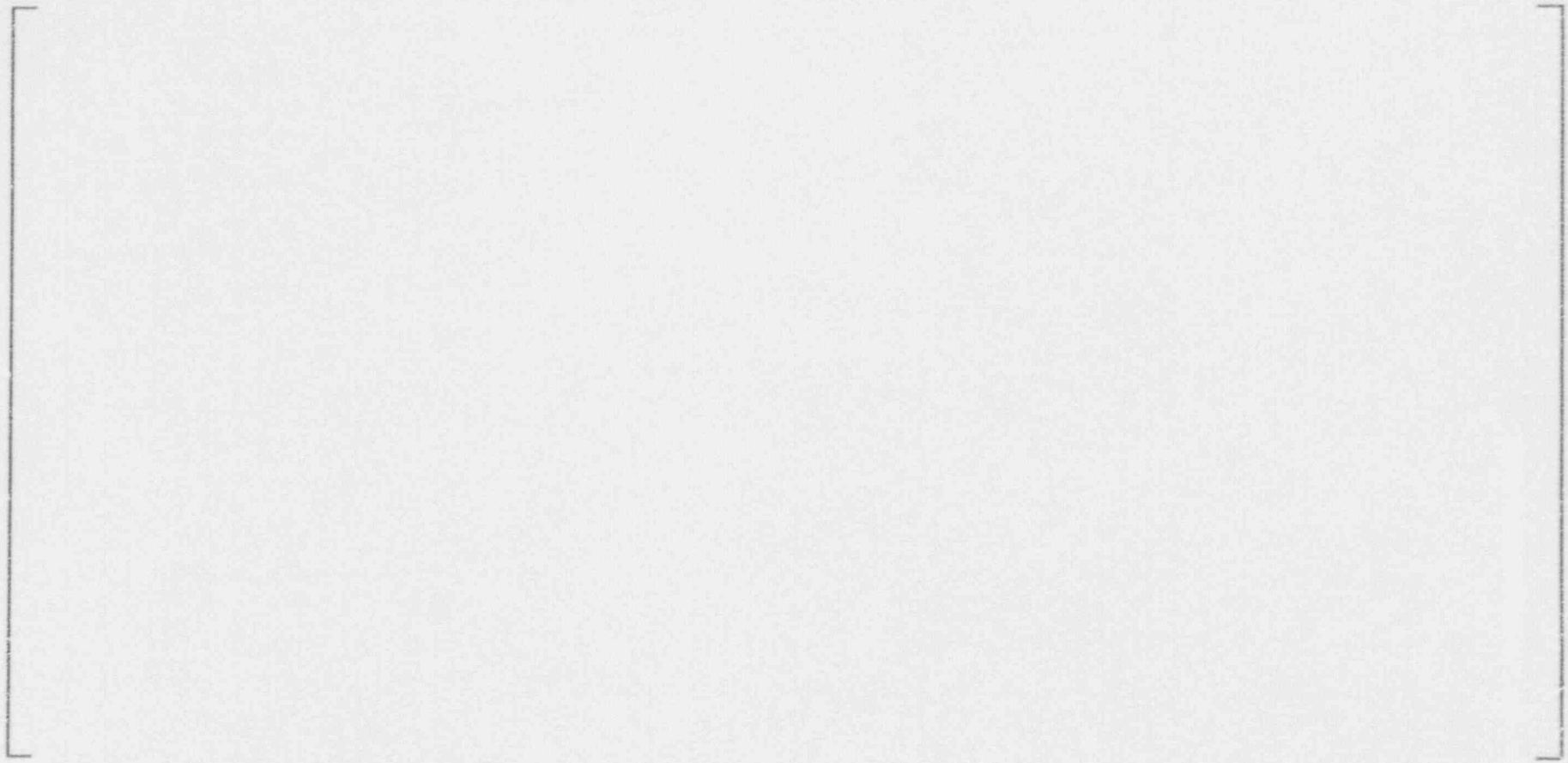

b,c

FIGURE 5-4

SEM MICROGRAPHS ILLUSTRATING
THE MICROSTRUCTURE OF THE
ALLOY 600 SAMPLE OBTAINED FROM
THE ST. LUCIE STATION PENETRATION
TUBE CALIBRATION STANDARD (BROMINE ETCH)

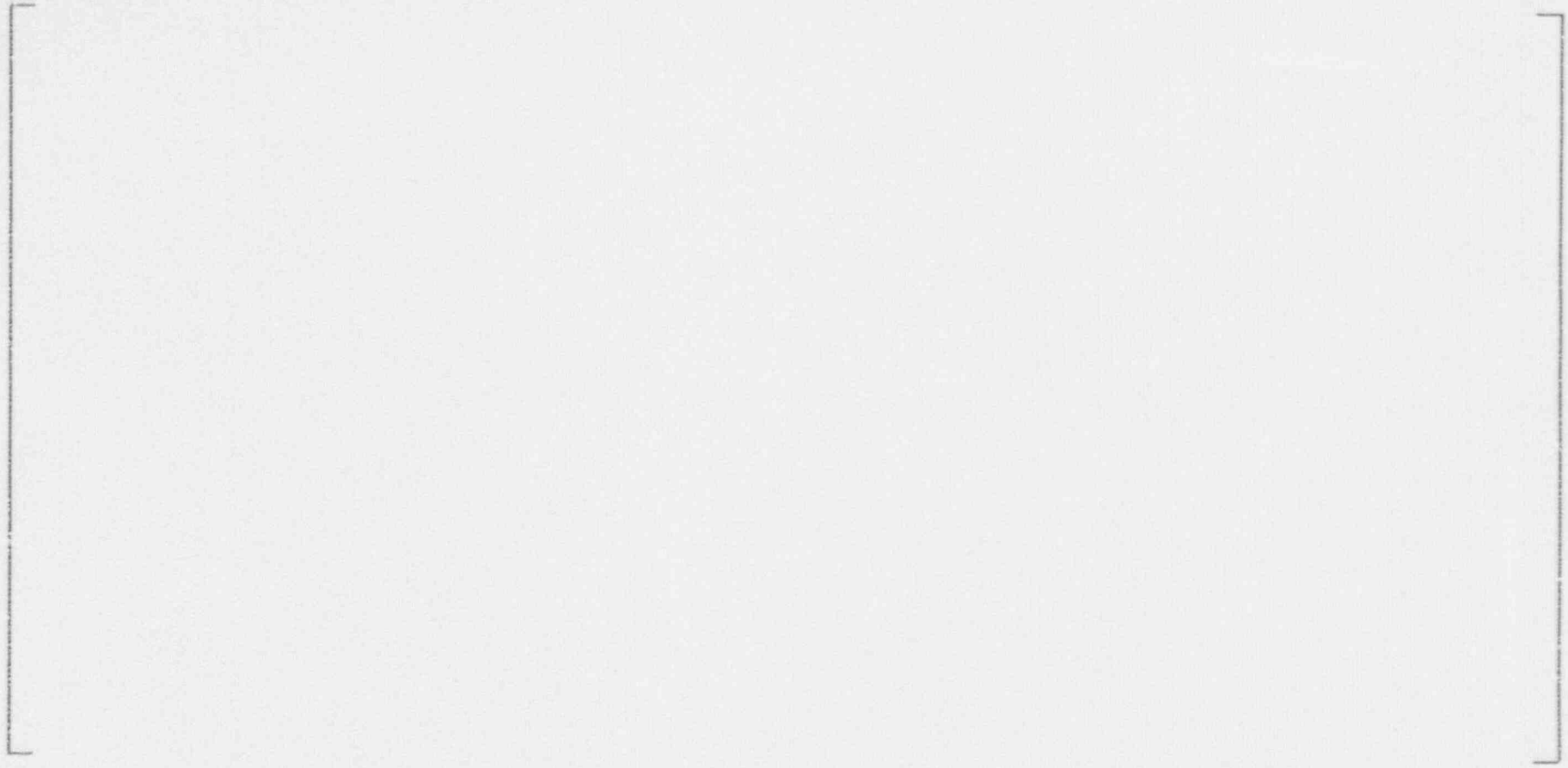

b,c

FIGURE 5-5

SEM MICROGRAPHS ILLUSTRATING
THE MICROSTRUCTURE OF THE
ALLOY 600 PENETRATION TUBE FOUND
IN THE JAMESPORT UNIT 1 REACTOR
VESSEL CLOSURE HEAD (BROMINE ETCH)

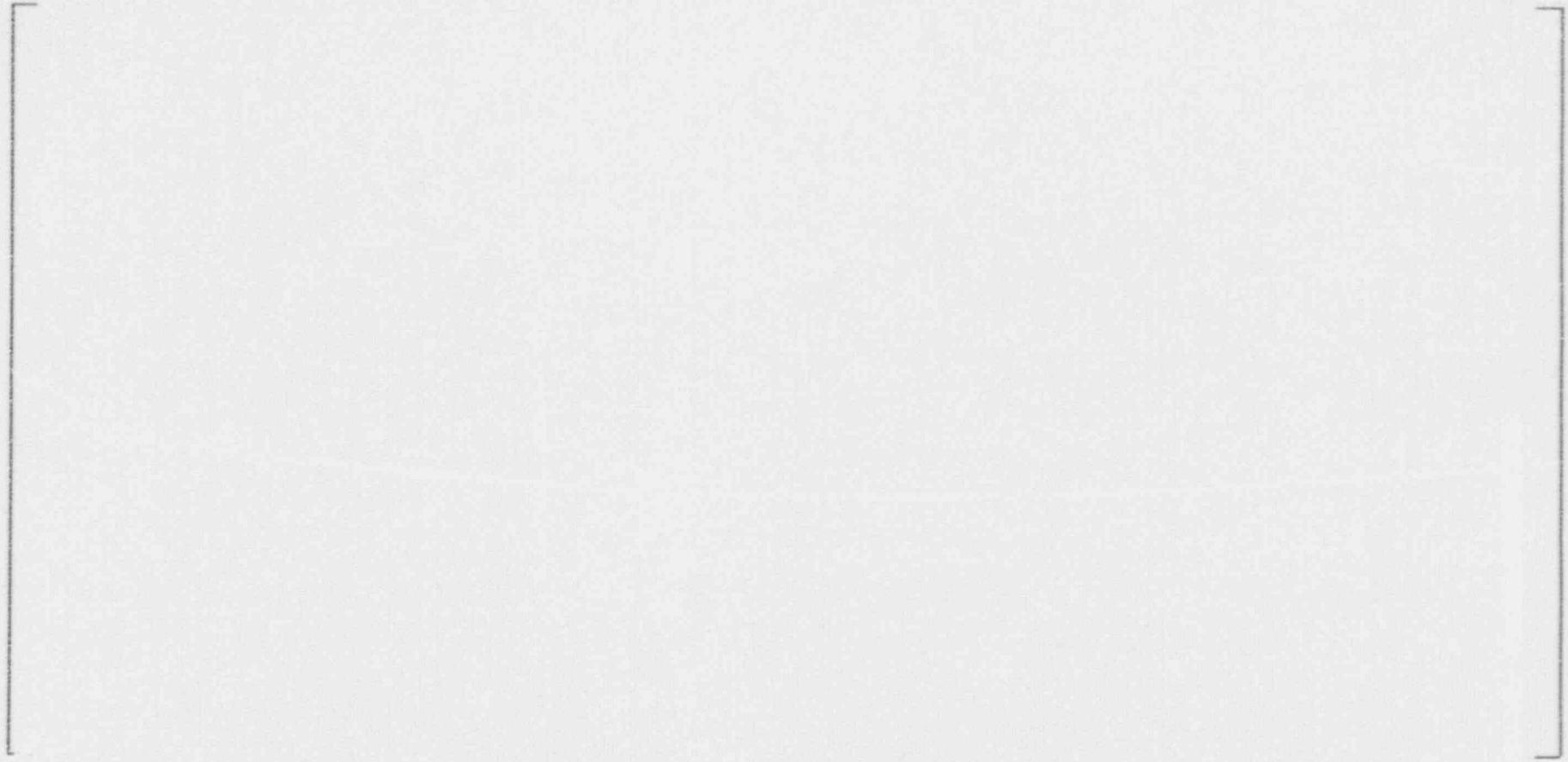

b,c

FIGURE 5-6

SEM MICROGRAPHS ILLUSTRATING
THE MICROSTRUCTURE OF THE
ALLOY 600 SAMPLE OBTAINED FROM
THE BRAIDWOOD STATION PENETRATION
TUBE CALIBRATION STANDARD (BROMINE ETCH)

b,c

FIGURE 5-7

SEM MICROGRAPHS ILLUSTRATING THE MICROSTRUCTURE FROM A SPARE PIECE OF THE ALLOY 600 MATERIAL HEAT USED IN THE RINGHALS UNIT 3 REACTOR VESSEL HEAD PENETRATION TUBES (BROMINE ETCH)

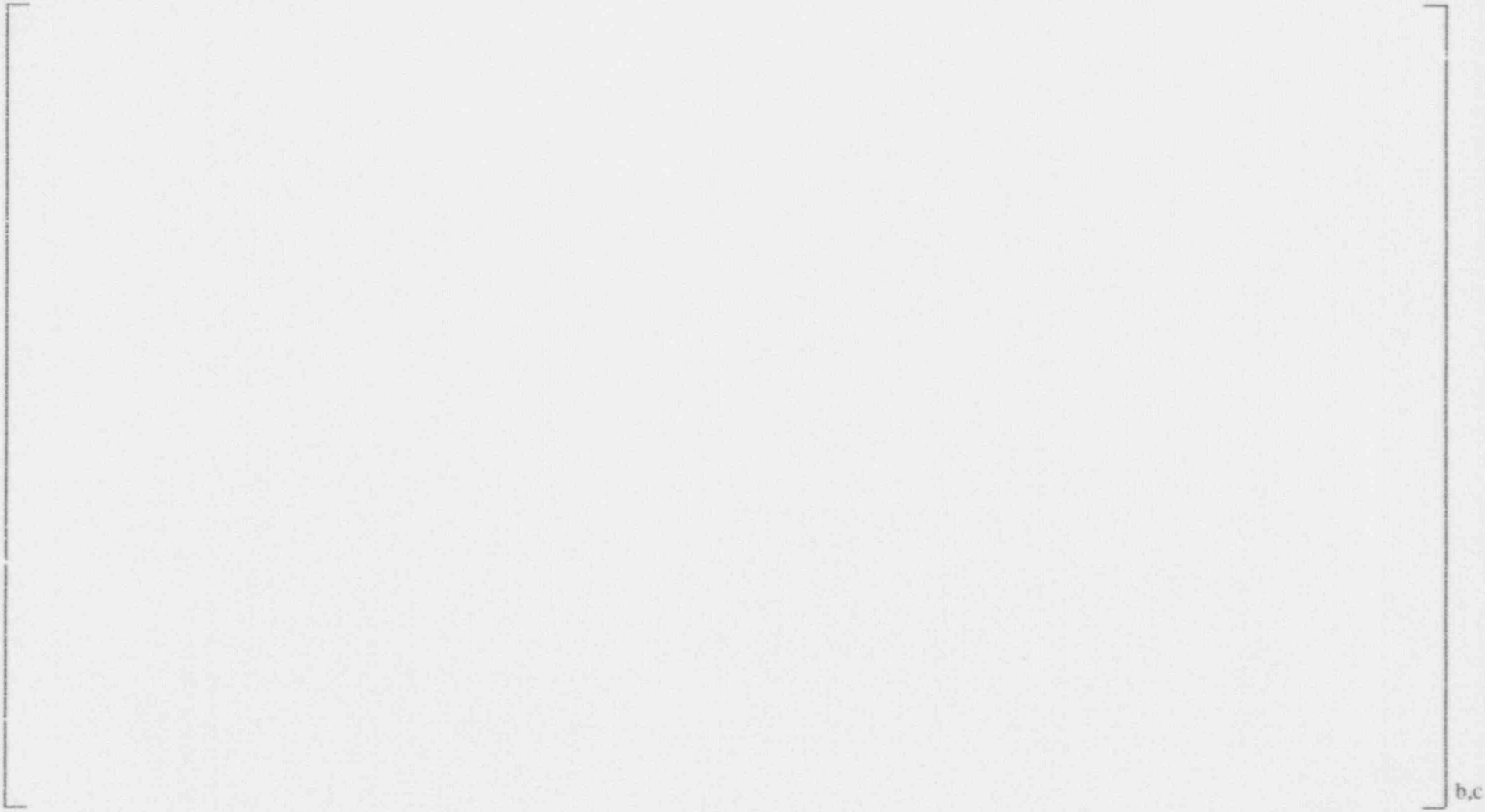

b,c

FIGURE 5-8
SEM MICROGRAPHS ILLUSTRATING THE MICROSTRUCTURE OF THE ALLOY 600 SAMPLE OBTAINED FROM THE BYRON STATION PENETRATION TUBE CALIBRATION STANDARD (BROMINE ETCH)

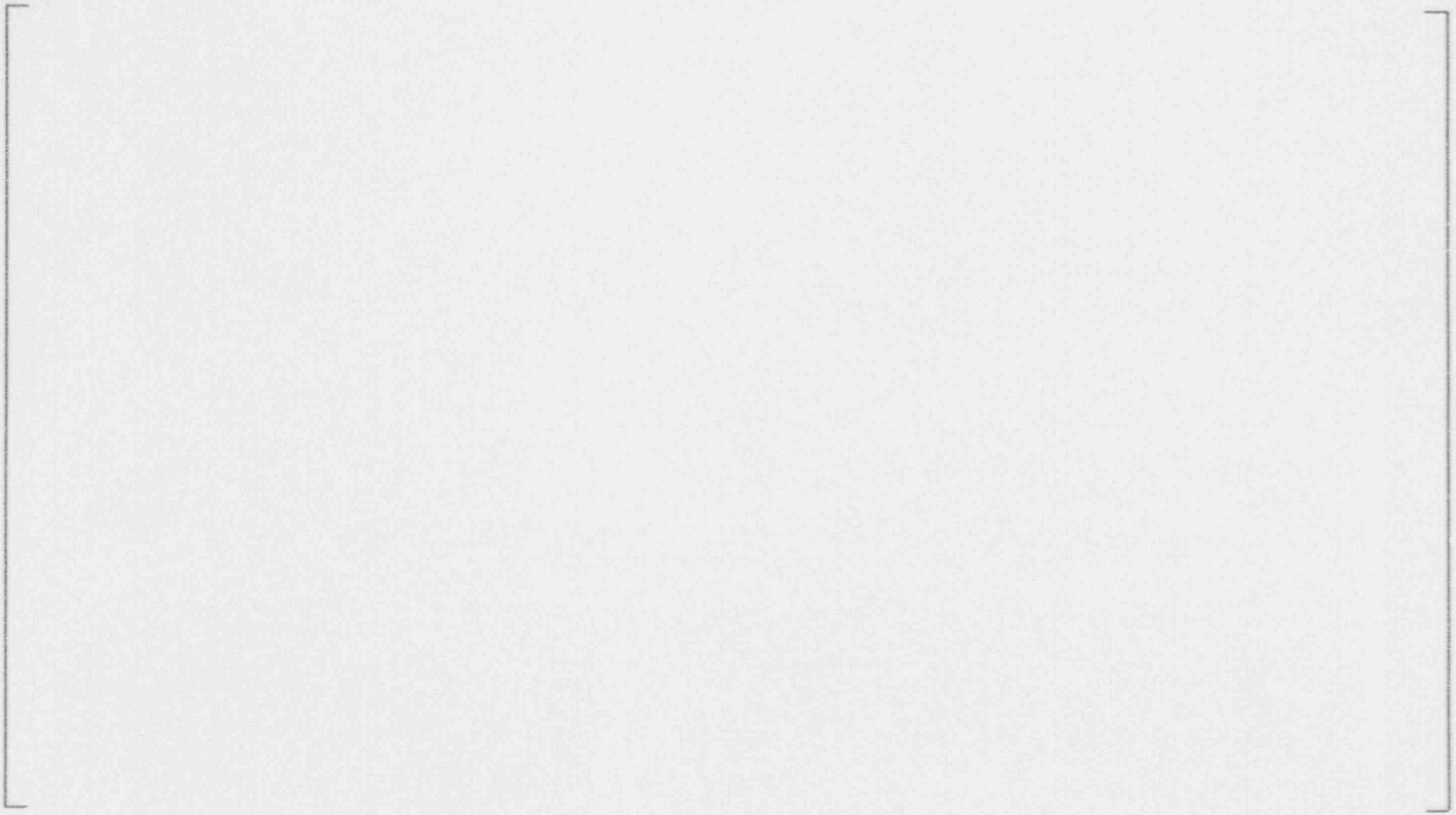

b,c

FIGURE 5-9
SEM MICROGRAPHS ILLUSTRATING THE MICROSTRUCTURE OF THE ALLOY 600 SAMPLE OBTAINED FROM THE WATTS BAR STATION PENETRATION TUBE CALIBRATION STANDARD (BROMINE ETCH)

6.0 References

[

]

C

[ ] c